



TRIBHUVAN UNIVERSITY
INSTITUTE OF ENGINEERING
PULCHOWK CAMPUS

THESIS NO.: M-385-MSREE-2021-2023

**Design and Improvement of Dewatering System Implemented for
Biogas Slurry**

By

Sunil Yadav

A THESIS

SUBMITTED TO

DEPARTMENT OF MECHANICAL AND AEROSPACE ENGINEERING

IN PARTIAL FULFILLMENT OF THE REQUIREMENT FOR

DEGREE OF MASTER OF SCIENCE IN

RENEWABLE ENERGY ENGINEERING UNDER

DEPARTMENT OF MECHANICAL AND AEROSPACE ENGINEERING

LALITPUR, NEPAL

NOVEMBER, 2023

COPYRIGHT

The author grants permission for this project report to be made freely available to public for study in library of Department of Mechanical and Aerospace Engineering at Institute of Engineering; Pulchowk Campus, Lalitpur, Nepal. The author acknowledges that permission to extensively reproduce this project report for academic purposes may be granted by the professor(s) who supervised the work described above, or in their absence, the Department Head.

The author and the Department of Mechanical and Aerospace Engineering at Institute of Engineering; Pulchowk Campus, Lalitpur, Nepal must be cited for any work derived from this project report. Without explicit permission of the author and Department of Mechanical and Aerospace Engineering at Institute of Engineering; Pulchowk Campus, Lalitpur, Nepal, the report cannot be used for any commercial purposes.

If anyone wishes to reproduce any portion of this project report, please contact the HOD of the Department of Mechanical and Aerospace Engineering at Institute of Engineering; Pulchowk Campus, Lalitpur, Nepal.

Head,

Department of Mechanical and Aerospace Engineering,

Pulchowk Campus, Tribhuvan University,

Institute of Engineering, IOE

Lalitpur, Nepal.

TRIBHUVAN UNIVERSITY
INSTITUTE OF ENGINEERING
PULCHOWK CAMPUS

DEPARTMENT OF MECHANICAL AND AEROSPACE ENGINEERING

The signatories hereby confirm that we have seen and given our approval of a project report titled "Design and Improvement of Dewatering System Implemented for Biogas Slurry" authored by Sunil Yadav. This project report has been submitted to Institute of Engineering, Pulchowk Campus for evaluation and recognition as part of the requisite coursework for a Master's in Renewable Energy Engineering. We certify that every information included in this project report has been created by the author and it does not contain any plagiarized material. We have provided guidance and supervision throughout the research and report writing process to ensure academic integrity and originality.

Date of Final Defence: 28th November, 2023

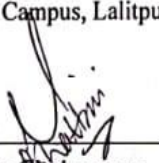
Supervisors,



Dr. Ajay Kumar Jha
Associate Professor,
Department of Mechanical and Aerospace
Engineering,
Pulchowk Campus, Lalitpur, Nepal.



Dr. Hari Bahadur Darlami
Associate Professor,
Program Coordinator of MSREE,
Department of Mechanical and Aerospace
Engineering.



Committee Chairperson
Dr. Sudip Bhattarai, Head of Department,
Department of Mechanical and Aerospace
Engineering,
Pulchowk Campus, Lalitpur, Nepal.



External Examiner
Doleshwar Koirala
Director,
Nepal Airlines Corporation.

ABSTRACT

The report titled "Design and Improvement of Dewatering System Implemented for Biogas Slurry" aims to validate the screw of existing dewatering machine initially created by Sherpa et al. in 2017 and modified by Sujan Jojiju in 2023. The goal is to validate the design, test the modified machine with effective screw press and evaluate its performance with respect to nutrient contents present in input and output materials along with comparison of its efficiency with conventional sun-drying process used in drying the slurry sample.

In Nepal, there is a significant demand for organic fertilizers and dewatering the biogas residue could serve as an eco-friendly alternative to chemical fertilizers. The design for validation of screw component and testing of machine are related to research, recommendations from literatures and advice from supervisors.

SolidWorks is used for the design process and ANSYS for the simulation works while its testing is conducted at workshop of GRIT Engineering Pvt. Ltd. The biogas slurry used for testing as well as sun-drying is collected from the biogas plant's prototype of 1m³ capacity present in the premises of Pulchowk Campus, Lalitpur. The machine's performance is evaluated at various operating speeds (36, 25, 20, 15, 10 and 8 rpm) using a Variable Frequency Drive (VFD). The results reveal that the most efficient operating speed being 8 rpm. The liquid yield, extraction efficiency, and extraction losses are determined to be 52.51%, 79.11% and 22.80%, respectively.

The slurry sample is sun-dried for 24, 48 and 72 hours whose nutrients concentrations (TS, N, P, K) are tested in Soil Water and Air Testing Laboratories Pvt. Ltd. The results show that optimum duration of sun-drying is 48 hours as its reduction of Total Solid contents is least. The slurry sample before testing in dewatering machine is also pre-treated for 24 and 48 hours to check the efficiency of existing machine and compare the results with that of sun-drying process.

From Financial analysis, the machine's installation cost is NRs. 392,000, along with the payback period, IRR and NPV are calculated as 1 year 10 months 23 days, 44% and NRs. 353575.86 respectively.

ACKNOWLEDGEMENT

At the very start, I'd want to offer my appreciation to the Mechanical and Aerospace Engineering Department, the Institute of Engineering (IOE) and Tribhuvan University for giving me with a chance to put my technical training to good use.

My deepest appreciation goes to **Dr. Ajay Kumar Jha** for his boundless enthusiasm and invaluable assistance with my thesis. I'd like to give special thanks to **Dr. Hari Bahadur Darlami**, the coordinator of the Master of Science in Renewable Energy Engineering, for giving inspiration of conducting the project works I needed to finish my thesis.

My deepest obligation goes out to Dr. Nawaraj Bhattarai and Dr. Laxman Paudel for their insightful comments. A debt of appreciation is due to following personnels: Er. Sujan Jojiju, Mr. Aditya Neupane, Mrs. Sabita Pradhan and Er. Dipesh Paudel. As for the testing of the machine, as well as their helpful practical advices, I'd like to give credit to GRIT Engineering Pvt. Ltd.

The entire Department has been very supportive of me as per thesis work; hence I am very appreciative of all they have done to help me succeed. I extend my sincere gratitude to the University Grants Commission (UGC), Nepal for precious provision on succeeding this research project. I also express gratitude to the Energize Nepal (Project Title: Clean Energy generation using Duckweed & PID: ENEP-RENP-II-22-03) and Centre for Pollution Studies (CPS), IOE, Tribhuvan University for their invaluable funding support and enabling the efficacious accomplishment of this project.

TABLE OF CONTENTS

COPYRIGHT	ii
ABSTRACT	iv
ACKNOWLEDGEMENT	v
TABLE OF CONTENTS	vi
LIST OF TABLES	ix
LIST OF FIGURES	x
LIST OF SYMBOLS	xi
LIST OF ABBREVIATIONS	xiii
CHAPTER ONE: INTRODUCTION	1
1.1 Background	1
1.2 Problem Statement	2
1.3 Objectives	2
CHAPTER TWO: LITERATURE REVIEW	4
2.1 Biogas Slurry	4
2.2 Review of Journal/Research Papers	4
2.3 Different Dewatering Technologies	9
2.4 Types of Screw used in screw press dewatering machine	10
2.5 Drying Technology of Digested Slurry	11
2.6 Performance Measuring Techniques	12
2.6.1 Moisture Content	13
2.6.2 Dry Matter	13
2.6.3 Extraction Yield, Extraction Efficiency and Extraction Loss	13
2.6.4 Dewatering Efficiency and Dewatering Rate	14
2.6.5 Separation Efficiency and Nutrient Loss Efficiency	14
2.6.6 Solid and Liquid Content with Effective Time required for drying	14
CHAPTER THREE: METHODOLOGY	15

3.1 Literature Review.....	15
3.2 Selection of appropriate technology and design software	16
3.3 Design calculations for further modelling and simulation works.....	16
3.4 Modeling of Dewatering System	18
3.4.1 Parts and Assembled Models	18
3.4.2 Modeling of screw presses.....	22
3.5 Simulation Works	23
3.6 Reliability Calculations.....	26
3.7 Performance Evaluation along with Nutrients Content Comparison.....	28
3.8 Results and Discussions.....	28
3.9 Conclusions and Recommendations	28
CHAPTER FOUR: DESIGN, STRUCTURAL AND CFD ANALYSIS ALONG WITH RELIABILITY CALCULATIONS.....	29
4.1 Design Calculations	29
4.2 Structural and CFD analysis in Software.....	31
4.3 Reliability calculations.....	34
CHAPTER FIVE: RESULTS FROM PERFORMANCE EVALUATION, NUTRIENTS CONCENTRATION ANALYSIS AND EFFICIENCY CALCULATION	35
5.1 Sun-drying Process	35
5.1.1 Results in terms of Nutrient Concentrations.....	35
5.1.2 Results in terms of Reduction Percentage	37
5.1.3 Results on Efficiency of Sun-drying Method	39
5.2 Combined Sun-drying and Dewatering process	40
5.2.1 Results on Nutrient Concentrations	40
5.2.2 Results in terms of Reduction Percentage	44
5.2.3 Results from Efficiency Analysis	47
5.3 Performance Evaluation of Dewatering Machine.....	48

5.4 Comparative Analysis	53
5.5 Time and cost efficiency Analysis	59
CHAPTER SIX: FINANCIAL ANALYSIS RESULTS AND DISCUSSIONS	60
6.1 Financial Analysis	60
6.2 Payback Period	61
6.3 Internal Rate of Return	62
6.4 Net Present Value	63
CHAPTER SEVEN: CONCLUSIONS AND RECOMMENDATIONS	64
7.1 Conclusions	64
7.2 Recommendations	65
REFERENCES	66
ANNEXES	69

LIST OF TABLES

Table 2.1: Four types of screw	10
Table 4.1: Results from structural analysis	31
Table 4.2: Pressure Contour from CFD simulation	32
Table 4.3: Velocity and turbulence kinetic energy from CFD simulation.....	33
Table 4.4: Summary of Reliability Calculations.....	34
Table 5.1: Results from Sun-drying method.....	35
Table 5.2: Reduction Percentage Calculation	37
Table 5.3: Results on Efficiency of Sun-drying process.....	39
Table 5.4: Results on Nutrient Concentrations	41
Table 5.5: Results as of Reduction Percentage	44
Table 5.6: Efficiency analysis	47
Table 5.7: Performance Results	48
Table 5.8: Results on Yield, Extraction Efficiency and Loss	51
Table 5.9: Comparison of solid form of slurry with compost.....	56
Table 5.10: Comparison of liquid form of slurry with comfrey liquid	57
Table 5.11: Results from Efficiency Analysis	58
Table 6.1: Annual Cash Flow	60

LIST OF FIGURES

Figure 2.1: Comparison of various artificial technology on the basis of TS	9
Figure 3.1: Methodology	15
Figure 3.2: Collector	19
Figure 3.3: Bearing	19
Figure 3.4: Pressure cone	19
Figure 3.5: Hopper	20
Figure 3.6: Covering	20
Figure 3.7: Sieve	20
Figure 3.8: Frame	21
Figure 3.9: Motor with screw press	21
Figure 3.10: Assembled model	21
Figure 3.11: Variable pitch screw with Straight shaft	22
Figure 3.12: Constant Pitch Screw with Tapered Shaft	22
Figure 3.13: Variable Pitch Screw with Tapered Shaft	23
Figure 4.1: Drawing of screw	29
Figure 5.1: Graph on RPM vs. Weight of solid cake extracted	49
Figure 5.2: Graph on RPM vs. Weight of Liquid Extracted	49
Figure 5.3: Graph on RPM vs. Weight of Liquid in cake	50
Figure 5.4: Graph on RPM vs. Extraction Yield	51
Figure 5.5: Graph on RPM vs. Extraction Efficiency	52
Figure 5.6: Graph on RPM vs. Extraction Loss	52
Figure 5.7: Weight Comparison	53
Figure 5.8: pH Value Comparison	54
Figure 5.9: Total Solids Comparison	54
Figure 5.10: Total Kjeldahl Nitrogen Comparison	55
Figure 5.11: Available Phosphorus Comparison	55
Figure 5.12: Available Potassium Comparison	56

LIST OF SYMBOLS

D_E	Dewatering Efficiency
D_R	Dewatering Rate
S_e	Separation Efficiency
NL_e	Nutrient Loss Efficiency
N_2	Nitrogen
M	Mass
ρ	Density of Slurry
V	Volume
H	Height
L	Length
R	Radius
W	Weight
T	Thickness
T_m	Torque
v_m	Velocity
N	Speed
Ψ	Filling coefficient
Π	pi (3.1416)
Q	Rate of Production
TA	Total Area
Σ	Summation
P	Power

μ	Coefficient of friction
N_f	Normal Reaction force
S_{ut}	Ultimate Strength
S_e	Endurance Strength
%	Percentage
TS	Total Solids
N	Nitrogen
P	Phosphorus
K	Potassium

LIST OF ABBREVIATIONS

AEPC	Alternative Energy Promotion Center
TS	Total Solids
RPM	Revolution Per Minute
NRs	Nepalese Rupees
CFD	Computational Fluid Analysis
MC	Moisture Content
DM	Dry Matter
Wt.	Weight
2D	Two Dimensional
3D	Three Dimensional
TSA	Total Surface Area
TKE	Total Kinetic Energy
Max	Maximum
Min	Minimum
E_y	Extraction Yield
E_l	Extraction Loss
E_e	Extraction Efficiency
TKN	Total Kjeldahl Nitrogen
IRR	Internal Rate of Return
NPV	Net Present Value

CHAPTER ONE: INTRODUCTION

1.1 Background

A biogas plant is straightforward, inexpensive and uncomplicated way to sustain energy supply since it allows for natural breakdown of organic ingredients without use of air. The question of whether the biogas slurry need to be dewatered and dried before using it in agriculture is raised, which can be utilized as a high nutrient fertilizer as it also does not impact the environment.

In Nepal, 316 large-scale biogas plants and 433,173 domestic or residential ones have been built around the nation. (AEPC, 2021). Similar to this, the Government of Nepal's 15th periodic plan aims to install an extra 200,000 home biogas plants along with 500 larger type of biogas plants. (15th periodic plan, 2019/20). As per AEPC, the imported dewatering system for cow-dung based slurry has been implemented by the industries located at Pokhara, Chitwan, Dhading and Biratnagar. Those are imported from country like, Italy, India, etc. and because of which they are seemed to be expensive technology in Nepal. Slurry production at the biogas plant is very prospective. The relevance of applying bio-slurry to the crops has been dominated by high manorial value of slurry that the crops may easily get. Slurry's dewatering is a treatment method to lower the moisture content of output slurry. Dewatered slurry can be transported, stored, controlled and used for a variety of applications since it can be treated as a solid rather than a liquid.

Dewatering is a crucial physical process, whether achieved naturally or mechanically, aimed at reducing the moisture content and volume of sludge. Its primary objectives encompass enhancing the sludge by increasing the dry substance content to around 40%, thereby making it more manageable and effective for various applications. This reduction in volume also leads to cost savings in transportation. Additionally, dewatering aids in improving the overall handling and transportation of the sludge while helping to mitigate odors, making it more environmentally friendly. Furthermore, by reducing humidity, dewatering increases the calorific power of the sludge, rendering it more useful for energy generation and other purposes.

1.2 Problem Statement

The slurry from a biogas plant naturally contains high moisture levels, making it challenging to handle, manage, and transport. Due to the lack of dewatering technology, the use of slurry is typically limited to the vicinity of the biogas plant, and even then, its quality may suffer. When slurry storage is required for an extended period, it can emit unpleasant odors. Most often, slurry is deposited near biogas plants, attracting mosquitoes, houseflies and other pests while emitting foul smells. Therefore, there is a need for technology that can expedite sludge replacement and allow for instant use of slurry as fertilizer. Using slurry as organic manure for cultivating crops can significantly reduce the reliance on imported fertilizers. Traditional methods of slurry dewatering are time-consuming and demand extensive storage space, making it impractical for commercial purposes. Imported technologies tend to be costly, emphasizing the necessity of establishing effective, locally available resource-based solutions for slurry treatment. The utilization of slurry not only reduces expenses on imported fertilizers but also contributes to the sustainability of biogas technology in rural energy systems. It not only saves traditional fuel resources but also decreases the demand for chemical fertilizers to some extent. Currently, the reliance on chemical fertilizers and the limited availability of rock phosphate poses a significant challenge. These fertilizers are susceptible to leaching and fail to efficiently provide phosphorous to plants. To mitigate this problem, organic sources like cow dung, which contain phosphorous, need to be incorporated into soil. However, the challenge lies in effectively utilizing biogas slurry derived from cow dung as a sustainable alternative. (Maneka Sanjay Gandhi, 2014)

1.3 Objectives

Main objective is to perform design and improvement of a screw press-based dewatering system with respect to sun drying method that is effective in lowering the moisture content of biogas slurry as well as conducting a financial analysis to ascertain the system's economic feasibility.

Specific objectives of this study are

- To design and simulate the main part of screw press based dewatering system like screw to get the complete model of efficient system
- To conduct performance evaluation of the dewatering machine on the basis of decreased moisture content of biogas slurry sample when it is combined with sun-drying method
- To analyze the TS, N, P, K contents on the biogas slurry sample collected from biogas plant after they get processed with sun-drying first and then combined sun-drying with dewatering
- To perform the financial evaluation of the dewatering technology for further real field application

CHAPTER TWO: LITERATURE REVIEW

2.1 Biogas Slurry

The biogas plant produces slurry as a byproduct of anaerobic digestion. The generation of biogas via anaerobic digestion is being investigated as a renewable energy source. In addition to biogas, this procedure produces slurry from undigested substrate. The slurry contains more than 90% water, making it difficult to transport from the production site to the farms. However, it is rich in plant nutrients (nitrogen, phosphorus, potassium, and micronutrients), which help plants grow and soil fertility. (Arora K. & Sharma S., 2016)) The nutrients like Phosphorus, potassium, zinc, iron, manganese and copper are all present in the biogas slurry. The slurry that has been digested includes 1.6% nitrogen (N), 1.55% phosphorus (P), and 1.00% potassium (K), whereas the composted slurry is made up of 0.75% N, 0.65% P, and 1.05% K. (Karki A. B., 2006)

The biogas-slurry's applications are:

- To improve both the quality and output of organic fertilizer at the farm level
- To apply it to plant roots in liquid form (diluted) or to plant leaves in dry form, and in composted form to ensure crops have adequate water
- To get nutrient constituents as: Nitrogen (N) which encourages the development of leafy greens as well as general plant's vigor; along with Phosphorus (P), that is crucial for developing healthy roots, flowers and fruits in plants; and Potassium (K) which increases a plant's resistance to disease, improve water absorption along with its general health

2.2 Review of Journal/Research Papers

Title	Author	Main Features
Design and Development of	(Chitte P. G., Tapsi P. & Deshmukh B. B., 2022.)	It was found in this research that upgrading from a single screw press to a twin screw press improved separation efficiency and product quality in the agricultural & food processing

Dewatering Screw Press		industries. These industries previously used a variety of methods, such as membrane filtration to produce nutrient concentrates from processed water and partial processing through simpler solid-liquor separation to produce digestate.
Designing a small-scale screw press for black water dewatering	(Morath Benjamin, 2023)	The final prototype was created by utilizing sheet pieces of stainless-steel metal. This allowed for the adoption of straightforward and economical manufacturing processes. Other components were created via additive manufacturing, which made it possible to realize more intricate designs of screw at minimal cost. The outcomes demonstrated that such a machine was capable of producing solids with a higher solid concentration of up to 30.3 wt.%.
Balancing operator input and cost - a case study for dewatering technology selection	(Goss C. T., Alsanea A., West J., Barry M., & Marx J., 2019)	Examining centrifuges, belt filter presses (BFPs), and screw presses were part of the assessment. Screw presses were chosen after taking into account operator preferences, safety considerations, worries about pathogen regrowth in centrifuge cake, increased odors in centrifuge cake and advice from expertise on other technical facilities with similar equipment.

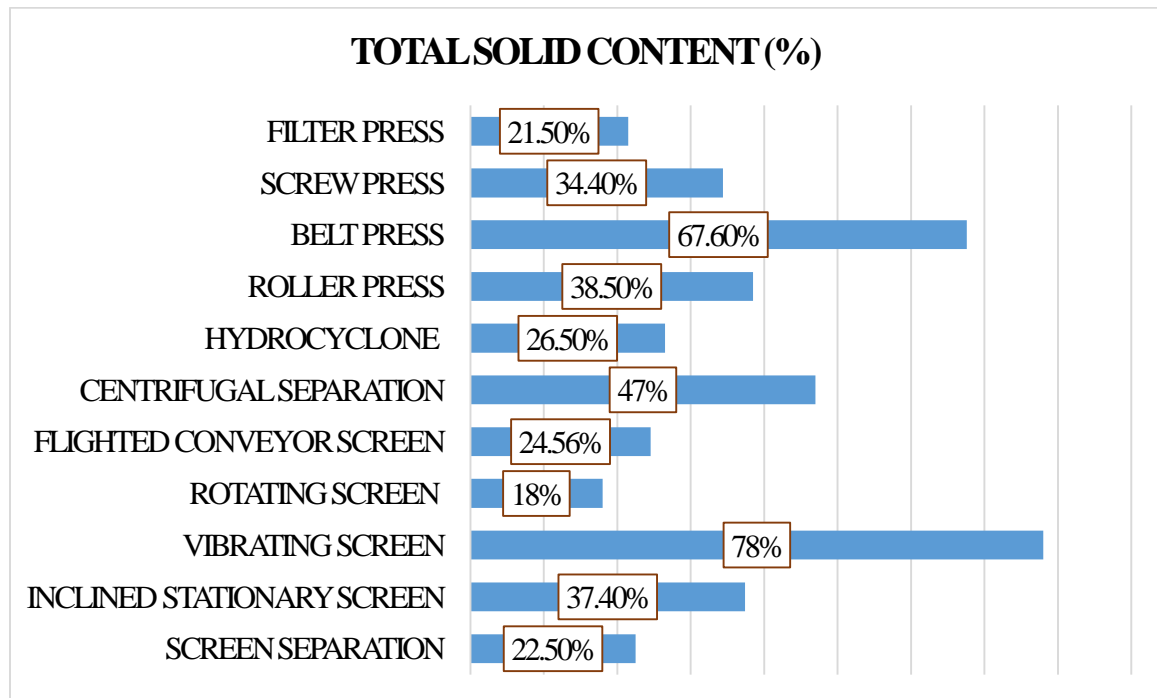
An Interactive Analysis of Influencing Factors on the Separation Performance of the Screw Press	(Fu S., Dou B., Zhang X. & Li K., 2023)	The findings showed that for the technology of screw press, following are most crucial for figuring out the water extraction rate: rotation speed > starting water content > back pressure. The production priorities for screw presses: rotational speed is greater than starting amount of water and back pressures. The ideal set of parameters produced 48.9% moisture removal and 234.2 kg/d of production with a 55% beginning water content, 30 r/min (speed of screw) and 5kPa (back pressure at exit).
CFD applied to decanter centrifuges	(Bhat A., 2023)	In this experiment, the flow of municipal sewage slurry inside a decanter centrifuge had been modeled using computational fluid dynamics (CFD). The decanter centrifuge's rotation was modeled using a sliding mesh technique, and the surface of the centrifuge drum was subjected to a moving wall boundary condition to approximate the speed difference.
Nutrient Recovery by Biogas Digestate Processing	(Bernhard Drosge et. al, 2015)	It became possible to handle manure, sewer sludge, wastewater and digestate in different ways. Membranes filtered water and produced enhanced nutritional concentrations. Cost-effective partial processing used decanter centrifuges and screw presses for solid-liquid separation. Complete processing needed specialized equipment and considerable energy usage, raising expenses. New digestate nutrient recovery strategies might improve agricultural and waste management. Standardization was

		also used to commercialize digestate-processed organic fertilizers.
Filtration of biogas spent slurry and its chemical analysis	(Er. Rahul Kadam, Dr. Deepak Sharma & Er. Ashish Pawar, 2017)	The advantages of waste-slurry as a crop fertilizer were significantly diminished when N ₂ was lost as ammonia after drying up to 90% of the water content. Several benefits were associated with utilizing the liquid component of the slurry after the solids had been removed, whether it was in a biogas plant. The processed slurry included 0.8 to 1.2% phosphorus, 1.5 to 2.0% nitrogen, and 0.8 to 1.0% potash.
Development of Screw Press-Dewatering Unit for Biogas Slurry	(M. More, C. Agrawal and D. Sharma, 2023)	Research first collected the biogas sludge by anaerobic digestion. Biogas slurry was expensive to transport and store as organic manure. Therefore, the screw press unit dewatered the biogas slurry into solid and liquid parts. Dewatering efficiency and rate were measured for the generated unit. When the biogas slurry had 80-85% moisture and the shaft speed was 40 rpm, Treatment (T9) achieved 81.82% dewatering efficiency. Treatment (T2) achieved 49.38 kg per hour at 85-90% moisture and 30 rpm shaft speed. Moisture and shaft speed affected solid-liquid separation.
End use diversification of biogas plant through design fabrication and	(P. Y. Sherpa, P. Sharma and R. Panthi, 2017)	The report focused on creating a machine for the purpose of dewatering the biogas slurry in Nepal to convert livestock waste into organic fertilizer. This innovation aimed to improve rural access to fertilizers and boost farmers'

testing of prototype biogas Slurry dewatering machine for mass dissemination in Nepal		income. The machine, designed in SOLIDWORKS and fabricated at Bishwas Engineering Works, was tested at Nilkantha Cow Farm. Results indicated that an operating speed of 10 rpm achieved optimal dewatering, with liquid yield of 91.39%, extraction efficiency of 80.177%, and extraction losses of 20.17%. The machine, powered by a 1 HP motor, produced 16.4 kg/hr of liquid.
Design, Fabrication and Performance Evaluation of The Dewatering Machine for Bio-Digestate	(Sujan Jojiju, 2023)	The report aimed to enhance a bio-digestate dewatering machine based on Sherpa et al.'s 2017 design, subsequently fabricating it for performance evaluation. The goal was to address Nepal's fertilizer needs by replacing imported chemical fertilizers with organic alternatives. Modifications were made using SOLIDWORKS, fabricated at GRIT Engineering Works Pvt Ltd, and tested with slurry collected from the Organic Farm House, Kapan. The key changes included a 5 HP motor, spring assembly, and a sieve. Performance tests at various speeds, managed by a Variable Frequency Drive, revealed a capacity of 79.90 kg/hr. The optimum operating speed was 10 rpm, with liquid yield at 90.77%, extraction efficiency at 71.64%, and extraction losses at 26.30%. It is possible to handle manure, sewer sludge, wastewater, and digestate in different ways.

2.3 Different Dewatering Technologies

Dewatering methods for sludge can be categorized into two main approaches. The first is natural dewatering, which relies on gravity settling and porous surfaces. This often takes the form of sludge drying beds, where liquid gradually evaporates into the atmosphere. The second approach is mechanical/artificial dehydration, which involves using machinery and processes to remove moisture from the sludge.



(M. Ford and R. Fleming, 2002)

Figure 2.1: Comparison of various artificial technology on the basis of TS

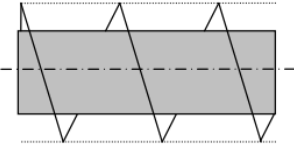
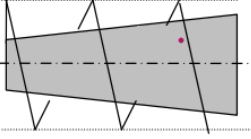
Screw presses efficiently dewater so that, such machines can be utilized in numerous production processes since they separate particles from liquids. Screw press dewatering devices use less energy than other varieties, lowering their lifetime operating cost (Emerging Technologies for Biosolids Management, 2006). A screw press dewatering machine requires less maintenance since it has fewer moving components. Limited capacity and high startup cost are the machine's main drawbacks (Riedel D. J., 2009). Based on this investigation and results, a Screw Press dewatering machine can be considered as the most beneficial item to design. Also, the Screw Press Dewatering

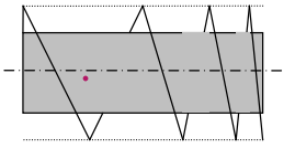
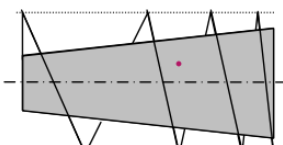
technique preserves more nitrogen, phosphorus, and potassium in output solids than other systems. Its minimal energy consumption and solids removal make it a good alternative for dewatering and nutrient retention. Nutrient preservation may reduce output solids compared to Centrifuge or Belt Press Dewatering. Therefore, the option should balance nutrient preservation with solids separation depending on the application's needs and objectives. (Bernhard Drosch et. al, 2015)

2.4 Types of Screw used in screw press dewatering machine

Biogas Slurry is compressed and dewatered using a screw press which is considered as main part of system. Screws are used to adjust the tension or location of mechanical elements. They come in a variety of sizes & forms comprised of materials including steel, brass or plastic. (Muhammad Firdaus et. al., 2017)

Table 2.1: Four types of screw

 <p>Constant pitch screw (Straight shaft)</p>	<p>The pitch and root diameter of particular screw press design remain unchanged throughout the screw press. Pressure levels may rise linearly. The screw press's process flow is continually replenished after each press stroke during a pressing.</p>
 <p>Constant pitch screw (Tapered shaft)</p>	<p>The circular area gets smaller as the screw goes along, and it's smallest at the very end. To find the volume that the screw thread moves during each spin, increase the pitch distance by the area of a circle.</p>

 <p>Variable pitch screw (Straight shaft)</p>	<p>When this screw shaft system turns, it takes up a little less area, kind of like a tapered shaft system. The rate at which pressure builds up through each thread is the primary distinction between them.</p>
 <p>Variable pitch screw (Tapered shaft)</p>	<p>It has a tapered shaft with a changeable pitch of screw. Because the pressure hits its highest point in fewer spins, it is possible to figure out the same amount of pressure in less time.</p>

2.5 Drying Technology of Digested Slurry

Drying of digested slurry is feasible when the rate of evaporation exceeds the rate of precipitation. The primary benefit is a substantial reduction in volume and weight, with the cost of constructing drying basins being relatively low. Slurry can also be dried on a stable surface near the plant overflow. During the drying process, pits or beds are periodically filled with slurry and removed once the desired moisture content is achieved. However, drying leads to a significant loss of inorganic nitrogen, up to 90 percent. Given the high moisture content of slurry (>90 percent), Sun drying is widely used in South Asia for treating the slurry, simplifying storage and enabling transportation with the application of dung. (Arora K. & Sharma S., 2016)

The drying time goes up as the thickness of the bed goes up. At a bed width of 10 cm, for example, it takes 20 days to lower the moisture level from 94% to 13%, which is too long to be useful. Similarly, a 7-cm thick bed needs 17 days to go from 93% moisture to 12% moisture, which means too much drying time and loss of nutrients (N, P, and K). At a bed

layer of 3.5 cm, the biogas spent slurry dries faster, in just 8 days, going from 88.63% to 21%. This makes it the best choice. Biogas waste may lose nitrogen as ammonia if it is dried until it is 90% dry. This makes it less useful as a field fertilizer. Getting the liquid part away from the solids makes it easier to reuse. The processed slurry usually has between 1.5 - 2.0% N, 0.8 - 1.2% phosphate and 0.8 - 1.0% potash. (Er R. Kadam, Dr. D. Sharma and Er. A. Pawar, 2017)

Drying rate relies on heat source temperature or irradiance, ambient air humidity, flow rate, and pressure, and exposed sludge surface area, thickness, and thermal characteristics (heat capacity and thermal conductivity). Radiative drying uses solar, infrared, microwave, or dielectric heat to evaporate moisture. Also, Solid fuel production from faeces requires drying. Drying increases net energy gains and decreases bulk, making it simpler to handle and lowering transportation costs. Passive drying using drying beds demands a vast footprint and weeks to months of occupancy. (Velkushanova K. Strande L. & Ronteltap M., 2021).

Eihe et al. (2019) found that acidified digestate (pH 6.5) cut NH_3 emissions by up to 90%, in contrast to digestate that wasn't acidified. Many establishments have discovered that drying digestate or the solid component is a cost-effective drying technology because it greatly reduces the amount of the product, making it better for export because it costs less to ship and store. (L. Morey, B. Fernández et. al., 2023). Cow dung used in this study has the following chemical properties: C/N ratio of 14.11, total nitrogen concentration of 2.12%, phosphorus concentration of 0.88%, potassium concentration of 3.54%, and pH of 8.23 were the measured values. Conditions at the experimental location were typically wet (during September & October) and dry (during November & February), with average temperature in the 26 to 34°C range. (Chutimanukul P., Iad-ak R. and Thepsilvisut O., 2023)

2.6 Performance Measuring Techniques

It is necessary to include both chemical qualities like N, P, and K in raw biogas slurry before and after dewatering, as well as a number of physical factors like pH value, moisture content, TS, etc.

2.6.1 Moisture Content

By comparing the weight of the slurry before and after drying, we can find out the amount of wetness is in the sample. So, sample's weight loss reveals the moisture content.

$$MC \text{ (in \%)} = \frac{B-C}{B-A} \times 100 \text{ (Nandi and Banik, 2000)} \quad (1)$$

Where, A= Wt. of vessel

B= Wt. of vessel + wt. of sample before dewatering

C= Wt. of vessel + wt. of sample after dewatering

2.6.2 Dry Matter

The quantity of water on any sample is represented by weight variance between the initial sample weight and end dry sample weight. The amount of DM is 100 less than the amount of water. (John K. Bernard, 2016)

$$\text{Dry Matter, DM (in \%)} = 100 - \left(\frac{\text{initial wt.} - \text{dry wt.}}{\text{initial weight}} \times 100 \right) \quad (2)$$

2.6.3 Extraction Yield, Extraction Efficiency and Extraction Loss

$$\text{Extraction Yield, } E_y = \left(\frac{W_{ce}}{W_{fs} + W_{lc}} \right) \times 100\% \quad (3)$$

$$\text{Extraction Efficiency, } E_e = \left(\frac{W_{ce}}{x \times (W_{lc})} \right) \times 100\% \quad (4)$$

$$\text{Extraction Loss, } E_l = \left(\frac{W_{fs} - (W_{ce} + W_{le})}{W_{fs}} \right) \times 100\% \quad (5)$$

Where, W_{ce} = Wt. of cake extracted (solid form)

W_{fs} = Wt. of feed sample

W_{lc} = Wt. of liquid in cake

x taken as 0.75 i.e., liquid content in slurry sample as 0.75. (Hussein Y. A., Alenyorege E. A. & Adongo T. A., 2015)

2.6.4 Dewatering Efficiency and Dewatering Rate

It is found by dividing the weight of the liquid that can be extracted out of slurry due to the extraction process by weight of actual raw form of slurry. (M. More, C. Agrawal and D. Sharma, 2023)

$$\text{Dewatering Efficiency, } D_E = (W_1/W_2) \times 100 \quad (6)$$

It is a measure of how much liquid is removed from new biogas slurry per unit of time.

$$\text{Dewatering Rate, } D_R = (W_1/T) \times 100 \quad (7)$$

Where, W_1 : Wt. of liquid extracted from raw form of slurry (kg),

W_2 : total wt. of slurry (kg),

T: Time needed at dewatering (hr).

2.6.5 Separation Efficiency and Nutrient Loss Efficiency

$$\text{Separation Efficiency, } S_e = [\{(TS)_{\text{output}} - (TS)_{\text{output}}\} / (TS)_{\text{output}}] \times 100 \quad (8)$$

Nutrient Loss Efficiency:

$$NL_e = [\{(Nutrient\ Contents)_{\text{input}} - (Nutrient\ Contents)_{\text{output}}\} / (Nutrient\ Contents)_{\text{input}}] \times 100 \quad (9)$$

2.6.6 Solid and Liquid Content with Effective Time required for drying

$$\text{Solid Content (\%)} = [(Initial\ Weight - Final\ Weight) / (Initial\ Weight)] \times 100 \quad (10)$$

$$\text{Liquid Content (\%)} = 100 - \text{Solid Content (\%)} \quad (11)$$

$$\text{Effective Time required for drying the sample} = (Initial\ Weight - Final\ Weight) / (\text{Rate of Drying}) \quad (12)$$

Where,

$$\text{Rate of drying} = (Initial\ Weight - Final\ Weight) / (Final\ Period - Initial\ Period)$$

CHAPTER THREE: METHODOLOGY

The process begins with a Literature Review, followed by Selection of appropriate technology and parts, then Design Calculations. Next is Modeling & Assembly in SolidWorks, Simulation in ANSYS, Performance Evaluation with Efficiency and Nutrient Content Comparison leading to Results and Discussions, and concludes with Conclusion and Recommendation. These flows of methods are stated as details given below.

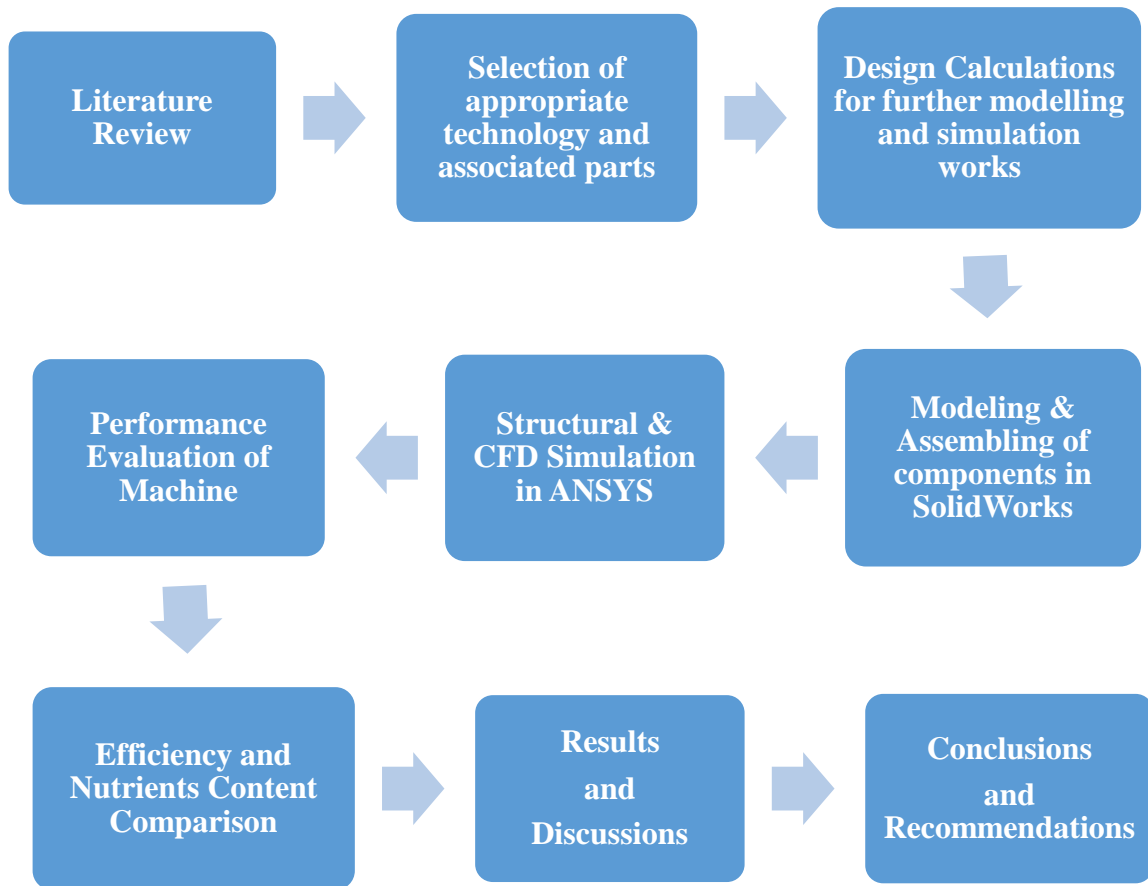


Figure 3.1: Methodology

3.1 Literature Review

The step of reviewing the literatures is continued with the research study. Various design parameter, guidelines for the design and installation of dewatering technology are studied.

The current use of pattern of biogas slurry management in Nepal are assessed and implication of the dewatering technology for drying of slurry are also analyzed. Literature reviewing involves systematically evaluating and summarizing existing research, publications and resources relevant to a specific topic. It helps identifying gaps in knowledge, build on previous findings and also provide context for new research or projects.

3.2 Selection of appropriate technology and design software

Finding the best material i.e., structural steel for a given systematic application of desired mechanical components is accomplished by evaluating their qualities, such as strength, durability and affordability. In order to ensure the best outcomes and efficiency, choosing software entails selecting a program that best suits project requirements, such as SolidWorks for design or ANSYS for simulations. Choosing the best technology for a work or project entails selecting the tools, systems or processes that are most appropriate for the work while taking efficiency, compatibility, cheap and innovation into account.

3.3 Design calculations for further modelling and simulation works

An essential project step, design calculations involve mathematical evaluations to verify accuracy and viability. The project's structural integrity, performance, and safety are guided by the parameters they specify for dimensions, forces, power required and other factors. These calculations serve as the basis for simulations, improving the accuracy and efficacy of the project design and analysis process as a whole. The formulas utilized for this calculation process include:

$$\text{Density of slurry, } \rho_{slurry} = \frac{M}{V_i} \quad (1)$$

Volume of Hopper as frustum of a pyramid,

$$V_h = \frac{\pi}{2}(R^2H - r^2h) \quad (2)$$

Volume of hollow tapered cylinder section,

$$V_1 = \frac{\pi \times l}{3} [(R_s^2 + R^2 + R_s \times R) - \{(R_s^2 + R^2 + R_s \times R) - t\}] \quad (3)$$

$$\text{Volume of Shaft, } V_2 = \pi R_s^2 l \quad (4)$$

$$\text{Mass of shaft, } M_s = \rho_s \times V \quad (5)$$

$$\text{Net Volume of flights, } V_f = 13 \times \pi r_f^2 t \quad (6)$$

$$\text{Mass of the flight, } M_f = \rho_s \times V_f \quad (7)$$

$$\text{Total Weight, } W = M \times g \quad (8)$$

$$\text{Power required, } P_1 = W \times v_m \text{ (Okafor, Basil E., 2015)}$$

$$v_m = \frac{Tm \times N}{60} \quad (9)$$

Throughput capacity,

$$Q\left(\frac{kg}{hr}\right) = \frac{60\pi D^2 Tm N \psi \rho_{slurry} c}{4} \text{ (Okafor, Basil E., 2015)} \quad (10)$$

Here, c = correction factor (0.7),

ψ = filling coefficient (0.125 for high abrasive materials)

Power required to convey the slurry,

$$P_2 = \frac{QL\rho_{slurry}F_{mt}}{168547} \text{ (Okafor, Basil E., 2015)} \quad (11)$$

Power required to press and separate slurry,

$$P_3 = F \times v_m \quad (12)$$

Where, F = Force required to separate the slurry = Squeezing pressure \times TSA in contact with slurry

Total area of flights,

$$TA_f; = \text{Sum of Area of 13 flights} = \sum[(\pi \times R^2) - (\pi \times r^2)] \quad (13)$$

$$\text{Force Required, } F = \text{Pressure} \times A_f \quad (14)$$

$$\text{And, } A_f = \left(\frac{TA_f}{2} \right)$$

$$\text{Frictional force, } F = \mu N_{fr} \quad (15)$$

$$\text{Motor Power, } P_m = P + (10\% \times P) \quad (16)$$

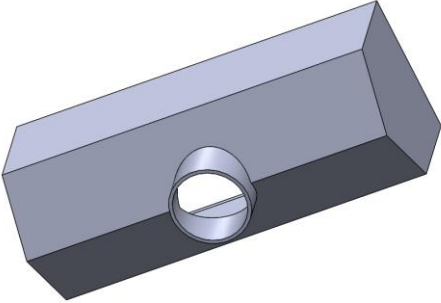

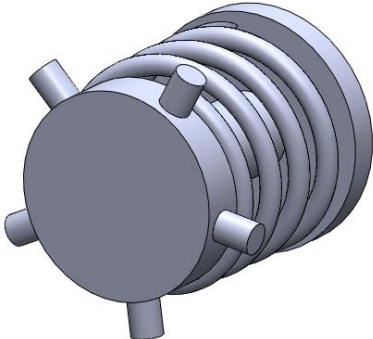
Where, P =Total Sum of Power

3.4 Modeling of Dewatering System

The modeling of the system is carried out by utilizing the features available in SolidWorks Software. First, the specifications and dimensions of the associated parts are understood. Then, reference drawings, images, and relevant information are gathered. SolidWorks is opened and a new part document is created. A 2D sketch is created by sketching on the desired plane by using sketch tools like lines, circles, arcs, and rectangles to outline the basic shape of the part. The dimensions are added to the sketch for specifying the sizes and positions of sketch entities. The extrude features are used to give depth and turn it into a 3D shape. The extrusion distance is specified with its direction by using various features like extrude, revolve, sweep, loft etc. to add or remove material and create the desired shape. Fillets are then added to round off edges and corners, and chamfers to create beveled edges. The threads and holes are modelled by hole-wizard and mirror features or bodies to create symmetric parts. Appropriate materials are assigned to the respective parts for analysis and visualization purposes. Finally, the parts file is saved with a descriptive name and organized it within a folder structure.

3.4.1 Parts and Assembled Models

The main parts of dewatering system are: bearing, collector, frame, hopper, motor with drive, screw rotor press, rectangular covering and pressure cone. These components are modelled in SolidWorks software and their 3D models with final assembled model are figured out as follows. Their dimensional drawings are stated in the annex part.

Name of Modelled Parts	Explanations
 <p data-bbox="492 688 763 724">Figure 3.2: Collector</p>	<p data-bbox="979 279 1417 751">After the water has been sorted from the solids that have been dried, it is collected by a collector. It guarantees effective drainage and makes water removal easier. Design and placement of the collector are essential for efficient water and output products management.</p>
 <p data-bbox="500 1178 753 1213">Figure 3.3: Bearing</p>	<p data-bbox="979 777 1417 1297">Bearings support rotating parts like shafts, guaranteeing smooth motion and reducing friction. For the system to operate consistently, the right bearing selection is essential. Bearings facilitate component movement and reduce wear during dewatering processes, both of which contribute to effective performance.</p>
 <p data-bbox="462 1816 787 1852">Figure 3.4: Pressure cone</p>	<p data-bbox="979 1329 1417 1686">In dewatering devices, pressure cone increases pressure on the mixtures for enhancing liquid drainage and solid concentration. This increases the effectiveness of dewatering and produces a denser solid cake.</p>

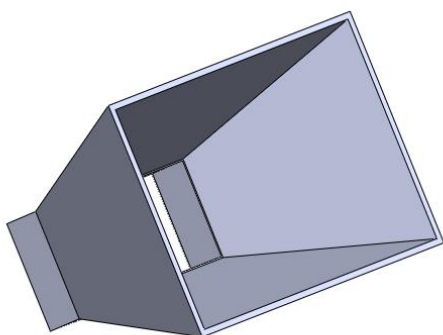


Figure 3.5: Hopper

A hopper is where material that is fed into a machine. Upon entering the hopper, the material is directed toward the machine's screw. It is an essential component since it makes loading efficient.

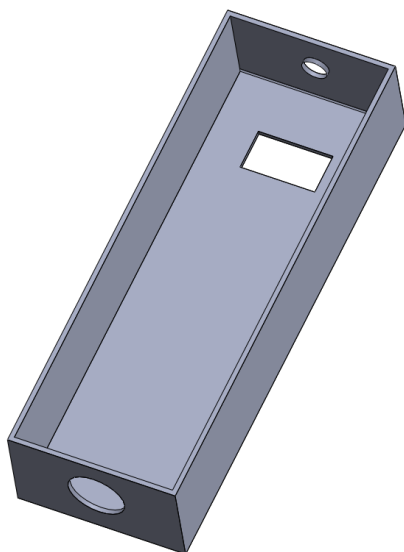


Figure 3.6: Covering

Covers keep the processed material contained and safeguard it. They keep the conditions ideal while dewatering operations are taking place and avoid contamination along with dust emission. A clean working environment, adherence to regulations, and general dewatering process efficiency are all aided by well-designed coverings.

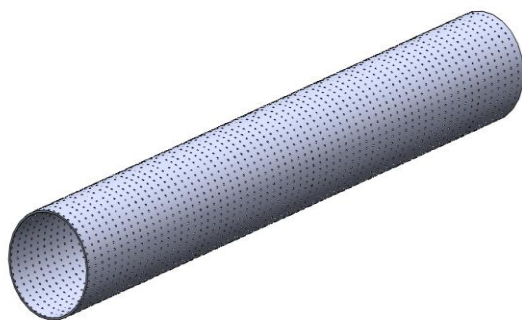


Figure 3.7: Sieve

A sieve or screen is used to separate the particles from the liquids during the dewatering stage of a screw press machine. With the help of a wire mesh, the sieve is designed to capture solid particles while allowing water to pass through it.

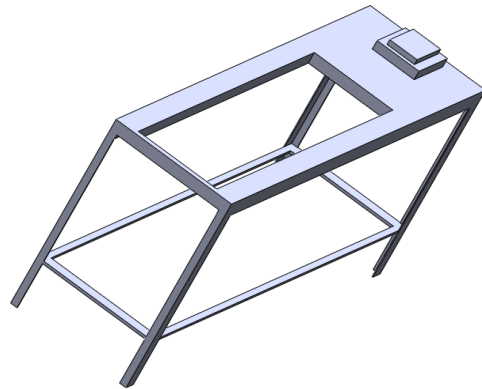


Figure 3.8: Frame

The frame of a screw press machine provides a sturdy structure to hold the numerous components of the machine and withstand the stresses generated during use. The frame is typically built out of steel or other robust materials that are strong, resilient, and deformation-resistant.

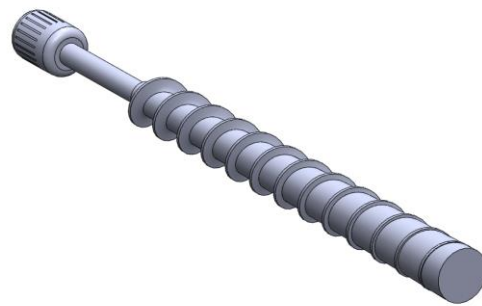


Figure 3.9: Motor with screw press

The motor and gearbox that make up a screw press machine's drive system are crucial parts because they provide the force and power needed to operate the screw press attached with the drive system.

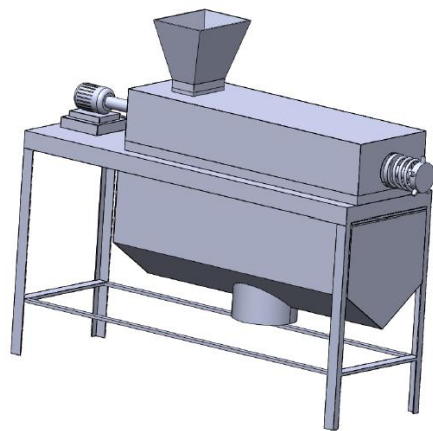

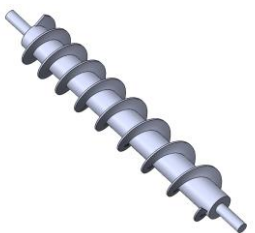



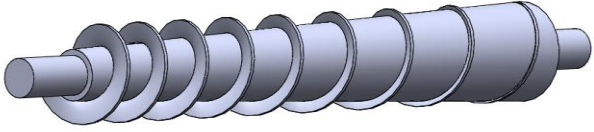
Figure 3.10: Assembled model

All the individual components are assembled into a single and complete model. It mainly represents the visual form of real machine used as dewatering system.

3.4.2 Modeling of screw presses

The four different types of screw presses are modelled in SolidWorks by following the similar sketching process as done for modelling the individual components of the dewatering machine. The layouts are given below:

Name of Modelled Parts	Explanations
 <p>Figure 3.11: Constant Pitch Screw with Straight shaft</p>	<p>A screw with a straight shaft and a constant pitch maintains constant thread spacing throughout its length. For applications needing continuous and predictable conveying or mixing processes.</p>
 <p>Figure 3.11: Variable pitch screw with Straight shaft</p>	<p>A straight shafted screw with variable pitch has varying thread spacing along its length. By progressively modifying the conveying or mixing action to account for varying flow rates and circumstances, this design optimizes material handling.</p>
 <p>Figure 3.12: Constant Pitch Screw with Tapered Shaft</p>	<p>A screw with a constant pitch and a tapered shaft maintains uniform thread spacing and has a gradual shaft taper. By accommodating varying flow rates and effectively transporting materials from one end to the other, this design improves material conveyance.</p>

 <p data-bbox="302 562 989 594">Figure 3.13: Variable Pitch Screw with Tapered Shaft</p>	<p data-bbox="1015 197 1419 827">The screw with a tapered shaft consists of changes in thread spacing and a gradual shaft as tapered. This design allows flexible material handling by modifying the dynamics of the conveying or mixing process in response to shifting flow rates. It is needed to process bulk materials effectively and flexibly under a variety of situations.</p>
---	---

3.5 Simulation Works

In ANSYS, simulation work entails the systems' parts to forecast their real-world behavior. To examine elements like stress, fluid flow and thermal performance, 3D models are used. To improve product dependability and performance, designs concepts are validated and engineering decisions are made with the use of simulation tools in ANSYS. To predict the response of system parts towards their endurance strengths, ANSYS performs structural simulations. Through the analysis of fluid flow, CFD simulations offer information on pressure and velocity management while the real field operations of mechanical system.

3.5.1 Static Structural Analysis

This analysis is started by importing the geometry of structure to be analyzed within the ANSYS software. After, the material properties are defined at the structure, such as Poisson's ratio and density. Meshing of imported geometry involves dividing the geometry of a structure into smaller nodes of 22669 and elements of 11951 in numbers, allowing numerical analysis to be performed on discrete parts having the min. edge length of 6mm. Similarly, Boundary conditions are applied to the screw presses models whose values are Moment of 3e+005N-mm along with fixed support at opposite end that prevents the part from moving. After that, loads, pressures and forces are applied to simulate the real-world

conditions. The solver settings are configured by specifying the analysis type (static). By which, the solver is run to perform analysis based on displacements, stresses, strains and other relevant static responses. Similarly, Post-processing tools in ANSYS are used for visualizing and interpreting the results in relation to stress contours or displacement plots.

Total Deformation

Total Deformation refers to the total displacement or shape change that a structure or item experiences as a result of external loads or forces. It takes into consideration all deformations, including displacements caused by translation and rotation. The overall deformation using ANSYS software in contour plots or graphical representations, show how the object's size and shape have changed as a result of applied loads. ANSYS contour plots interpret blue and red colors differently depending on the analysis stages and values visualized. The maximum limit serves as an indicator to identify areas with potential weaknesses highlighting regions of excessive deformation. Conversely, minimum limits help pinpoint locations with minimal deformation aiding in the identification of critical stress zones and informing feasible design improvements.

Equivalent Stress

Equivalent Stress refers to a single value that combines a variety of stresses acting on a material or structure. It is a streamlined measurement that incorporates different stress elements, including hydrostatic stress, normal and shear stress for depicting the impact of stress condition on the material's failure potential. The mathematical formulas that address the intensities and interactions of various stress components are used by ANSYS software to determine equivalent stress. The maximum contour serves as a tool to identify vulnerable locations at risk of material failure prompting the need for structural reinforcement. Conversely, the minimum limit directs attention towards areas with minimal stress aiding in design optimization and the establishment of safety margins.

Equivalent Elastic Strain

Equivalent Elastic Strain refers to a single value that sums up all of the strain that a material experiences under the effect of applied loads with both the normal & shear components of strain. Using a formula that accounts the magnitudes and interactions of various strain

components, ANSYS calculates equivalent elastic strain. The strain is useful in anticipating the behavior of materials, patterns of deformation, and the possibility of structural failure. The value also ensures that materials are used safely within permissible strain limits. The maximum equivalent elastic strain assists in identifying areas nearing critical strain levels alerting to potential material failure. Meanwhile, the minimum limit highlights regions with minimal strain ensuring the structural integrity of the system.

3.5.2 CFD analysis

After importing the geometry and meshing them in the ANSYS software, the fluid properties including density, viscosity are defined & the fluid behavior such as turbulence models or multiphase interactions are specified. The respective boundary conditions including inflow or outflow velocities, pressures, temperature are applied to represent the interactions of fluid with the solid surfaces & its external environment. Then, the solver setting is configured by specifying the analysis type as steady-state or transient which solves the fluid flow equations for calculating velocity, pressure properties.

Fluid Flow Domain

Fluid flow domain is the physical region where fluid motion takes place. It includes all borders, surfaces, and volumes that are involved in fluid dynamics phenomena. Here, 105mm of outer diameter and 2400mm length of domain along with the flow rate of 0.55kg/s have been defined.

Pressure contour

The ANSYS program identifies a "pressure contour" as a visual depiction of the pressure distribution across a surface or object following analysis. It provides a color-coded diagram of the object that highlights the different pressure levels in different regions. Using this contour diagram, engineers and analysts can may better comprehend how pressure is distributed and varies across the structure. In fluid dynamics and other fields, it is a useful tool for locating regions of high or low pressure during the design of components. The maximum contour color restrictions serve as indicators of high-pressure regions, drawing attention to the risk of potential overloading. Conversely, the minimum limits highlight

areas with lower pressure aiding in the identification of suction zones or regions with reduced stress.

Velocity contour

In an ANSYS fluid or gas flow simulation, a "velocity contour" is a graphical depiction of the distribution of velocities. Different colors are used to show the various velocity magnitudes over the analysis domain. In domains like fluid dynamics, aerodynamics, and heat transfer, understanding the flow patterns of the fluid or gas at play is accomplished by emphasizing regions of greater or lower velocity. By providing a visual representation of the flow of fluids or gases inside a system, velocity contours facilitate the study along with development of several technological fields. The maximum contour color limits highlight regions with the highest TKE indicating intense turbulence. Conversely, the minimum limitation identifies areas with lower TKE signifying smoother flow conditions. This facilitates the analysis of turbulence impacts and optimization of designs for enhanced effectiveness and stability.

Turbulence Kinetic Energy

The term “TKE” refers to a quantity used to assess the energy associated with turbulent motion within a fluid flow in CFD simulations. TKE displays the level of turbulence throughout the flow field. The TKE distribution in a fluid domain is used to compute and visualize the contour plots or graphical representations for understanding of fluid behavior, heat transfer and other phenomena connected to fluid dynamics with the analysis of the turbulence aspects of flow. The maximum value draws attention to areas with potential turbulence or acceleration effects. Conversely, the minimum limit identifies stagnant zones. This information guides the optimization of designs for improved fluid dynamics and overall performance.

3.6 Reliability Calculations

The calculation is performed on the designed and simulated parts of four varied types of screw press for checking its reliability and sustainability at real field operations. The formulas associated with it are given below.

Factor of Stress Concentration,

$$K_t = \text{Ratio of Max. to Min. Equivalent stress} \quad (17)$$

$$K_f = 1 + q(K_t - 1) \text{ Where, } q=0.8 \quad (18)$$

$$\text{Reliability factor, } K_e = 1 / K_f \quad (19)$$

$$S_e' = 0.504 \times S_{ut} \text{ (where, } S_{ut} = \text{Ultimate strength)} \quad (20)$$

$$\text{Factor of size modification, } d = \sqrt{18^2 - 8^2} = 16.125 \quad (21)$$

$$K_b = 1.189 (d)^{-0.097} \quad (22)$$

$$\text{Endurance limit (MPa), } S_e = K_a. K_b. K_d. K_e. S_e'$$

Where, Surface modification factor, $K_a=0.765$;

$$K_b=0.908; \quad (23)$$

$K_d = 1$ (Temperature modification factor);

$$K_e=1$$

$$b = (-1/3) \times \log [(0.8 \times S_{ut}) / S_e] \quad (24)$$

$$c = \log [(0.8 \times S_{ut})^2 / S_e] \text{ (where, } S_{ut} \text{ in psi but } S_e \text{ in Mpa)} \quad (25)$$

$$\text{Total rotation of screw, } N = 10^{(-c/b)}. S_f^{(1/b)} \quad (26)$$

$$v = L \div 4.5 = 38.2905 \text{ mm/s (where, Distance of pitch, } L=172.307\text{mm)} \quad (27)$$

$$t = s/v = 29.250\text{sec (where } s=1120\text{mm)} \quad (28)$$

$$t_p = p/v = 4.179 \text{ sec (where, } p=160\text{mm)} \quad (29)$$

$$\text{Time to complete one cycle, } t_{\text{total}} = t + t_p = 33.429\text{sec} \quad (30)$$

$$\text{Total rotation within 1 hr., } N_p = 3600 / t_{\text{total}} = 107.692 \text{ rotation} \quad (31)$$

$$\text{Total life-span (hours), } L_t = N / N_p \quad (32)$$

3.7 Performance Evaluation along with Nutrients Content Comparison

After getting detail idea of detailed dimension of parts for assembled model and decision from the simulation, the fabricated system is used for the validation and performance testing of the screw press dewatering technology by utilizing the process of combined sun-drying with dewatering of the collected biogas slurry samples. The samples are collected from the biogas plant of 1m³ capacity. When the sun-drying process is performed, the sample is kept under sunlight during daytime for 24 hours, 48 hours and 72 hours of duration. And, the dewatering process also adheres the sun-drying as pre-treatment process for improving its efficiency and content of nutrients in sample. But when the pre-treatment process as of sun-drying for dewatering system takes place, the sample collected is kept in the form of bed having 4cm thickness at the sunlight of daytime for about 24 and 48 hours. Here, the energy of sunlight raised from the indirect radiation for all the durations have an average temperature of 26°C as well as an average solar irradiance of 5.3Wh/m².

3.8 Results and Discussions

Results are used to display data and observations that usually show the results of experiments, simulations, or analyses. Discussions assess the findings by contrasting them with predictions and earlier studies. These processes help in understanding the project's significance, coming to conclusions and determining areas that need more research or improvement.

3.9 Conclusions and Recommendations

The conclusion highlights accomplishments, limitations and consequences while summarizing the project's results and insights. By restating important ideas and listing the project's contributions to knowledge or useful applications, it offers closure. The conclusion helps put the project's significance and results to get effective process for combined form of sun-drying & dewatering and writing the further recommendations of project at various fields.

CHAPTER FOUR: DESIGN, STRUCTURAL AND CFD ANALYSIS ALONG WITH RELIABILITY CALCULATIONS

4.1 Design Calculations

Calculations for different components are carried out by the help of different theories & literatures that are used for checking the viability of designing the machine parts:

4.1.1 Design of hopper

The volume of hopper depends on density of slurry and mass of the slurry to be fed at a time. Let, the mass of slurry to be fed at once, $M=5\text{kg}$

Volume of slurry, $V_i=0.004545\text{m}^3$ ($M=5\text{kg}$, $\rho_{\text{slurry}}=1100\text{kg/m}^3$)

Hopper design is based on the volume of frustum of a pyramid. (J.K., Khurmi R.S. & Gupta, 2005)

$R = 125\text{mm}$; $H = 200\text{mm}$; $r = 80\text{mm}$; $h = 50\text{mm}$

Volume of the hopper, $V_h = 0.00406\text{m}^3$

4.1.2 Power needed to overcome the screw and shaft's motion

The shaft is tapered & made hollow.

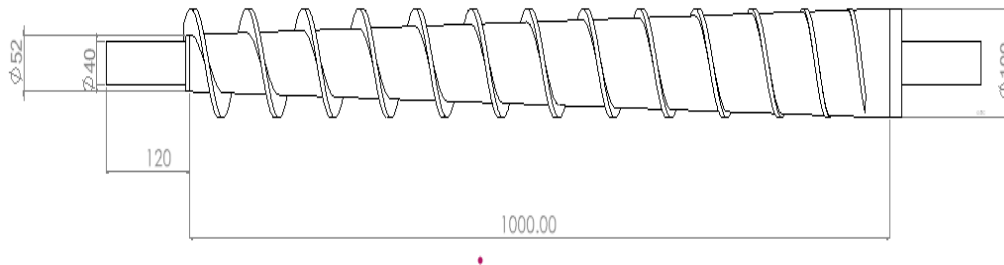


Figure 4.1: Drawing of screw

$V_1 = 0.000688009\text{m}^3$ [since, ($R=50\text{mm}$, $r=26\text{mm}$, $L=1000\text{mm}$, $R_s=40\text{mm}$, $t=6\text{mm}$)]

Volume of 40mm shaft, ($l=1.24\text{m}$)

$V_2=0.00155823\text{m}^3$

Total volume of shafts, $V = V_1 + V_2 = 0.002246239m^3$

$$M_s = 17.63kg \text{ } (\rho_s \text{ for mild steel} = 7850kg/m^3)$$

Radius of flights = r_f (50mm)

$$\text{So, } V_f = 0.00061261057m^3$$

$$M_f = 5.178kg$$

Total Mass, $M = M_s + M_f = 22.81kg$

$$W = 223.75N$$

$$v_m = 0.01216m/s$$

$$\text{So, } P_1 = 2.720 \times 10^{-3} \text{ kW.}$$

4.1.3 Power needed to convey the slurry

Firstly, the throughput capacity of the screw press is determined. $Q = 33kg/hr$

F_{mt} is the material factor per kW. So, $P_2 = 0.123kW$

4.1.4 Power Required to Press and Separate Slurry

According to (Mudryk, 2016), the optimum pressure required to separate biogas effluent slurry into solid and liquid constituents is approximately 1.74 MPa.

$$TA_f = 0.064251m^2$$

$$F = 0.45 \times 0.032126 = 14.45KN$$

$$P_3 = 0.175712KW$$

4.1.5 Power Required to Overcome Friction

$$\text{Frictional force, } F = 0.35 * 14.45 * \cos 30 = 4.3779KN$$

$$\text{Frictional Power, } P_4 = 0.05325kW$$

$$\text{Total Power required, } P = P_1 + P_2 + P_3 + P_4 = 0.3546828kW$$

4.1.6 Motor Selection

$$P_m = 0.390\text{kW} = 0.5229 \text{ hp.}$$

Hence, an electric motor is chosen with a power rating of 1 horsepower (hp) based on the formula, which calculates the motor's power requirement while accounting for 10% losses. This selection ensures the motor meets the specified power needs proficiently.

4.2 Structural and CFD analysis in Software

At first, the static as well as CFD analysis works are performed for all the four-screw press models whose results are obtained as described below.

Table 4.1: Results from structural analysis

Types of Screw and shaft	Deformation (mm)	Equivalent Stress (MPa)		Equivalent Strain (mm/mm)	
	Max	Max	Min	Max	Min
Constant pitch screw with Straight shaft	0.2129	46.19	0.0046493	0.00024385	3.6288e-8
Variable pitch screw with Straight shaft	0.21344	45.035	0.0083044	0.00022607	7.1824e-8
Constant pitch screw with Tapered shaft	0.17151	43.941	0.0259	0.00022244	4.1637e-7
Variable pitch screw with Tapered shaft	0.17116	46.285	0.048465	0.00023649	3.1202e-7

Here, the constant pitch screw with a tapered shaft exhibits the least deformation suggesting its superior structural integrity in the system. The variable pitch screw with a

tapered shaft follows closely in terms of low deformation slightly outperforming the constant pitch screw. Meanwhile, the constant pitch screw with a straight shaft and the variable pitch screw with a straight shaft both experience higher levels of deformation. Moving on to equivalent stress values, it is evident that the variable pitch screw with a tapered shaft experiences the highest stress indicating potential structural vulnerability in this configuration. The constant pitch screw with a straight shaft exhibits slightly lower stress levels, while the constant pitch screw with a tapered shaft shows the least stress implying its ability to handle loads effectively. The variable pitch screw with a straight shaft falls in between these stress values. Finally, considering equivalent strain, the constant pitch screw with a tapered shaft demonstrates the least strain followed by the variable pitch screw with a tapered shaft, the variable pitch screw with a straight shaft and the constant pitch screw with a straight shaft which exhibits the highest equivalent strain. In conclusion, the constant pitch screw with a tapered shaft appears to offer the most desirable combination of low deformation, stress and equivalent strain making it the optimal choice for this particular application.

Table 4.2: Pressure Contour from CFD simulation

Pressure (Pa)	Max	Min	Difference
Constant pitch screw (Straight shaft)	3.608e+001	-1.471e+000	37.551
Variable pitch screw (Straight shaft)	2.338e+001	-1.631e+000	25.011
Constant pitch screw (Tapered shaft)	8.258e+001	-7.585e+000	90.165
Variable pitch screw (Tapered shaft)	6.553e+001	-7.364e+000	72.894

The table presents a comparison of pressures generated by various screw press configurations. It is evident that the constant pitch screw with a tapered shaft exhibits the

highest pressure, while the variable pitch screw with a tapered shaft follows with slightly lower pressure. The constant pitch screw with a straight shaft shows lower pressure levels compared to the previous two and the variable pitch screw with a straight shaft demonstrates the lowest pressure among the configurations. Notably, a significant pressure differential of 90.165 Pa is observed in the constant pitch screw with tapered shaft scenario indicating substantial pressure variations along the tapered shaft. To ensure system stability and reliability, optimized case of pressure differentials in the Constant pitch screw with Tapered shaft arrangement is imperative.

Table 4.3: Velocity and turbulence kinetic energy from CFD simulation

Types of Screw and shaft	Velocity (m/s)		Turbulence Kinetic Energy (m ² /s ²)	
	Max	Min	Max	Min
Constant pitch screw (Straight)	9.280e-002	5.308e-003	2.912e-004	1.576e-005
Variable pitch screw (Straight)	9.235e-002	5.308e-003	2.907e-004	1.599e-005
Constant pitch screw (Tapered)	5.135e-002	5.308e-003	1.907e-003	2.399e-005
Variable pitch screw (Tapered)	5.139e-002	5.308e-003	9.165e-004	2.451e-005

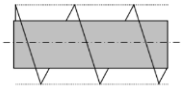
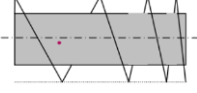
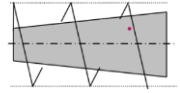
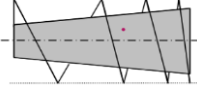
While comparing the maximum and minimum velocity ranges within a screw press featuring constant and variable pitch configurations, it becomes evident that the constant pitch screw with a straight shaft exhibits the highest velocity, followed closely by the variable pitch screw with a straight shaft. The variable pitch screw with a tapered shaft displays a lower velocity and the constant pitch screw with a tapered shaft demonstrates the lowest velocity among the configurations. When considering turbulence energy, the constant pitch screw with a tapered shaft stands out with the highest turbulence energy value. This configuration's superior turbulence energy characteristics, combined with its

lower velocity, make it a desirable choice for specific applications, as it balances flow dynamics efficiently ensuring optimal performance and reliability.

4.3 Reliability calculations

The reliability and sustainability of four different types of screw presses are assessed through calculations conducted on their designed and simulated components in order to evaluate their performances in real field operations.

Table 4.4: Summary of Reliability Calculations

 Constant pitch screw (Straight shaft)	 Variable pitch screw (Straight shaft)	 Constant pitch screw (Tapered shaft)	 Variable pitch screw (Tapered shaft)
$K_t = 9934.82$ $K_f = 7948.063$ $K_e = 0.00012581$	$K_t = 5423.03$ $K_f = 4338.424$ $K_e = 0.00023043$	$K_t = 1696.56$ $K_f = 1357.248$ $K_e = 0.000737$	$K_t = 955.019$ $K_f = 764.016$ $K_e = 0.001308$
$S_{ut} = 420\text{Mpa}$ $S_e' = 211.68\text{Mpa}$ (or 30693.6 psi) $S_e = 21324.493\text{ psi}$ $= 147.027\text{Mpa}$	$S_{ut} = 440\text{Mpa}$ $S_e' = 221.76\text{Mpa}$ (or 32163.627 psi) $S_e = 22339.945\text{ psi}$ $= 154.028\text{Mpa}$	$S_{ut} = 450\text{Mpa}$ $S_e' = 226.800\text{Mpa}$ (or 32894.618 psi) $S_e = 22847.671\text{ psi}$ $= 157.529\text{Mpa}$	$S_{ut} = 410\text{Mpa}$ $S_e' = 206.64\text{Mpa}$ (or 29970.652 psi) $S_e = 21324.493\text{ psi} =$ 143.526Mpa
S_f (fatigue case) $= 480\text{Mpa}$ $b = -0.840$; $c = 7.208$ $N = 244558.921$ $= 244.56 \times (10^3)$ rotations	$S_f = 480\text{Mpa}$ $b = -0.840$; $c = 7.228$ $N = 258482.480$ $= 258.482 (10^3)$ rotation	$S_f = 480\text{Mpa}$ $b = -0.840$; $c = 7.238$ $N = 265489.904$ $= 265.49 \times (10^3)$ rotation	$S_f = 480\text{Mpa}$ $b = -0.840$; $c = 7.198$ $N = 237643.947$ $= 237.644 \times (10^3)$ rotation
$L_t = 2270.913$ hours	$L_t = 2400.204$ hours	$L_t = 2465.273\text{ hours}$	$L_t = 2206.703\text{ hours}$

(I. Nawi, Z. Ngali, M. Firdaus, S.M. Salleh, E.M. Yusup & W.A. Siswanto , 2017)

CHAPTER FIVE: RESULTS FROM PERFORMANCE EVALUATION, NUTRIENTS CONCENTRATION ANALYSIS AND EFFICIENCY CALCULATION

5.1 Sun-drying Process

Firstly, sun-drying method is performed for reducing the content of moisture and also knowing the condition of nutrient contents present in the biogas slurry sample collected for the project.

5.1.1 Results in terms of Nutrient Concentrations

Nutrient concentrations (N, P, K) in biogas slurry (bio-digestate) are assessed through sun-drying process that yields the following results.

Table 5.1: Results from Sun-drying method

Experimental Parameters	Before Sun-drying	After 24 hours of Sun-drying	After 48 hours of Sun-drying	After 72 hours of Sun-drying
Weight (kg)	10.38	7.42	6.24	5.46
pH Value	6.9	5.4	5	4.8
Total Solids (%)	14.67	22.11	29.55	44.87
Total Kjeldahl Nitrogen, N (%)	0.3	0.26	0.21	0.09
Available Phosphorus, P (mg/kg)	89.67	86.73	83.79	81.48
Available Potassium, K (mg/kg)	1637.5	1317.5	997.5	860

Weight

Sun-drying cow dung slurry for varying amounts of time considerably reduces its weight. Before drying, the slurry has a weight of 10.38 kg. It falls to 7.42 kg after 24 hours in the

sun, 6.24 kg after 48 hours, and 5.46 kg after 72 hours. This pattern is indicative of the sun-drying process, which removes moisture to leave a more concentrated slurry with a greater proportion of solids. A decline in weight indicates that moisture has been extracted, which is desirable in many agricultural contexts.

pH Value

Slurry's pH value changes when it dries in the sun. The pH value of 6.9 is intermediate between an acidic state and a neutral one before drying. The pH of anything dried in the sun drops with time. After 24 hours, it decreases to 5, then after 48 hours it drops to 5, and after 72 hours it drops to 4.8. The concentration of acidic substances during drying is attributed to evaporation of water and the possible release of organic acids owing to microbial activity.

Total Solids

As the time spent in the sun increases, the total solids percentage in the slurry also rises. Total solids make up 14.67 percent of the slurry. This number increases to 22.11 percent after 24 hours in the sun, 29.55 percent after 48 hours, and 44.87 percent after 72 hours. Sun-drying's efficacy in lowering the slurry's moisture content and concentrating its solids is shown. A greater total solids percentage implies a more nutrient-dense slurry, which may be useful for enriching soil and growing plants.

Total Kjeldahl Nitrogen, N

When slurry is dried in the sun, its N-concentration changes. The TKN level is 0.3% before drying. It drops to 0.26 percent after 24 hours in the sun, 0.21 percent after 48 hours, and 0.09 percent after 72 hours of drying time. The drying process dilutes the nitrogen concentration, which explains why TKN content decreases. Although N-concentration drops, a substantial quantity of nitrogen is retained in the slurry, making it useful as an organic fertilizer.

Available Phosphorus, P

During sun drying, the slurry loses some of its phosphorus availability. There is 89.67 mg/kg of phosphorus accessible before it is dried. It drops to 86.73 mg/kg after 24 hours of sun drying, 83.79 mg/kg after 48 hours and 81.48 mg/kg after 72 hours. Because soluble

phosphorus molecules are lost as water is evaporated, the amount of accessible phosphorus decreases throughout the drying process.

Available Potassium

As the sun-drying process continues, the potassium level of the cow dung slurry falls. There is a total of 1637.5 mg/kg of potassium accessible before it is dried. The amount decreases from 1317.5 mg/kg to 997.5 mg/kg and then up to 860 mg/kg after being dried in the sun for 24, 48, and 72 hours, respectively. The concentration of potassium compounds during drying is responsible for the decline in accessible potassium content.

5.1.2 Results in terms of Reduction Percentage

Using the sun-drying technique, a sample of biogas digestate slurry is analyzed for changes in weight, pH, and content based on total soluble solids (TS), nitrogen (N), phosphorus (P), and potassium (K).

Table 5.2: Reduction Percentage Calculation

Reduction Percentage	Before Sun-drying	After 24 hours of Sun-drying	After 48 hours of Sun-drying	After 72 hours of Sun-drying
Weight (kg)	28.52	15.90	12.50
pH Value	21.74	7.41	4.00
Total Solids (%)	-50.72	-33.65	-51.84
Total Kjeldahl Nitrogen, N (%)	15.00	17.65	57.14
Available Phosphorus, P (mg/kg)	3.28	3.39	2.76
Available Potassium, K (mg/kg)	19.54	24.29	13.78

Weight

Sun-drying causes a change in mass, which may be seen in the weight loss percentage. As the material dries in the sun for 24, 48, and 72 hours, its weight gradually decreases from its peak. Weight loss occurs when water is evaporated from a substance during solar drying.

It's worth noting that the degree to which the substance loses weight shows the pace at which it dries out and gains concentration.

pH Value

The material's alkalinity or acidity may be deduced from this measurement. To start, the pH level remains rather constant. However, the pH of the substance significantly decreases when it dries in the sun. A significant drop in pH is seen after 24 hours, and this tendency is maintained at the 48- and 72-hour periods. The acidity of the material seems to rise as the pH drops during drying.

Total Solids

The TS in the slurry is having a varied reaction to sun-drying. Although the exact % reduction is not given at the outset, after 24 hours of sun-drying there is a considerable reduction in total solids. After 48 hours, the percentage of total solids indicates an increase, which might indicate that there is a fall in moisture content due to the drying process, followed by a rehydration impact.

Total Kjeldahl Nitrogen

Total Kjeldahl N-concentration percentage variations are significant. At first, there isn't much of a fluctuation in the nitrogen concentration. However, the concentration of nitrogen significantly increases after 24 hours of sun-drying, and it continues to climb at the 48- and 72-hour marks. This indicates that a high concentration of nitrogen occurs in the substance after sun-drying. The material's nutritional content and its potential use in agriculture and the environment may be modified by these processes.

Phosphorus

During sun-drying, there are notable shifts in the available phosphorus content. At first, it's quite steady. However, after 24 hours in the sun, there is a little increase in available phosphorus concentration. This trend lasts for the first 48 hours, then begins to wane during the next 72. The variation in phosphorus concentration may be due to changes in chemical makeup as it dries. It is important to understand these changes in order to evaluate the material's potential agricultural applications.

Potassium

The sun-drying procedure also causes some fluctuation in the total quantity of usable potassium. In the beginning, it's quite constant. However, after 24 hours in the sun, the amount of usable potassium rises dramatically. This trend, which has been rising over the last 48 hours, starts to stabilize after 72 hours. These shifts in potassium content are indicative of dynamic changes brought about by sun drying. Longer sun-drying improves the storage and handling but also result in lower nutrient content. So, for nutrient-rich fertilizer production, shorter drying times i.e., 48 hours is preferred.

5.1.3 Results on Efficiency of Sun-drying Method

The evaluations are conducted to determine results related to the efficiency of the sun-drying method by encompassing moisture content, dry matter, dewatering efficiency and dewatering rate.

Table 5.3: Results on Efficiency of Sun-drying process

Efficiency Measuring Parameters	Before Sun-drying	After 24 hours of Sun-drying	After 48 hours of Sun-drying	After 72 hours of Sun-drying
Weight (kg)	10.38	7.42	6.24	5.46
Moisture Content, MC (%)	0	28.79	16.12	12.70
Dry Matter, DM (%)	0	71.48	84.10	87.50
Dewatering Efficiency, D_E (%)	0	28.52	39.88	47.40
Dewatering Rate, D_R (%)	0	12.33	8.63	6.83

The data related to the dewatering process of bio-digestate over a span of 72 hours shows that the slurry initially weighs 10.38 kg before undergoing sun-drying. As the drying process progresses, several key parameters are measured. First, the MC of substance decreases significantly from 28.79% after 24 hours to 12.70% after 72 hours. Conversely, the dry matter content increases from 71.48% to 87.50% during the same time frame. This indicates a progressive reduction in the water content and an increase in the solid content of the substance. Dewatering efficiency is a crucial indicator, which shows the effectiveness of the dewatering process. It notably improves from 28.52% after 24 hours to an impressive .90% after 47.40 hours, demonstrating that the drying method becomes increasingly efficient over time. The rate at which water is removed from a solution is known as the dewatering rate (D_R). After 72 hours, the rate drops from 12.33% to 6.83 percent suggesting that the dewatering process is slowing down. In conclusion, the data shows that sun-drying approach is efficient in lowering the water content and raising the dry matter content of the material with rising dewatering efficiency and decreasing moisture content during a 72-hour period.

5.2 Combined Sun-drying and Dewatering process

Here, the combined sun-drying and dewatering process is performed to evaluate its effectiveness in reducing moisture content and assessing nutrient content in the collected biogas slurry sample for the project.

5.2.1 Results on Nutrient Concentrations

The performance of the combined sun-drying and dewatering process is assessed in relation to nutrient concentrations as N, P, K. Biogas slurry sample is a rich source of essential plant nutrients: nitrogen, phosphorus, and potassium. Nitrogen is vital for enabling plants to create proteins, crucial for developing green stems, robust roots, and abundant foliage. Phosphorus plays a key role in energy distribution within the plant, crucial for its maturation. Potassium is important for the synthesis of sugars necessary for plant growth, particularly beneficial for root crops. This combination of elements in cow dung slurry makes it an effective and valuable resource for plant health and further development.

Table 5.4: Results on Nutrient Concentrations

Experimental Parameters	Pre-treatment (Before Sun-drying)	Pretreatment (After 24 hours of Sun-drying)	Pretreatment (After 48 hours of Sun-drying)	After Dewatering (Solid Form)	After Dewatering (Liquid Form)
Weight (kg)	95.44	74.45	58.56	32.74	10.45
pH Value	8.4	8	7.9	7.8	7.6
Total Solids (%)	15.95	20.14	22.23	24.32	14.57
Total Kjeldahl Nitrogen, N (%)	0.36	0.39	0.41	0.42	0.31
Available Phosphorus, P (mg/kg)	81.48	76.16	73.05	70.84	79.59
Available Potassium, K (mg/kg)	1005	958.22	934.33	911.44	917.10

Weight

As the slurry of cow manure is processed further, its weight noticeably decreases. The slurry has an initial weight of 95.44 kg before being dried in the sun. After drying in the sun for 24 hours, the weight lowers to 74.45 kg, and after 48 hours, it falls to 58.56 kg. The solidified slurry weighs in at 32.74 kg of solid while 10.45kg of liquid after being

dewatered. The sun-drying and dewatering procedures accounted for the majority of the slurry's weight loss. Slurry loses weight because it gets more concentrated when water evaporates. This pattern illustrates the efficiency of sun-drying and dewatering in lowering the moisture content and raising the solids concentration in the slurry.

pH Value

The pH value of the slurry demonstrates a progressive fall as it passes through successive phases of processing. The first pH reading, taken before sun drying, shows an alkaline behavior at 8.4. After drying in the sun for 24 hours, the pH drops to 8, and after 48 hours, it drops even more to 7.9. The pH level remains constant at 7.8, following dehydration. Several things have contributed to the pH dropping to this level. When water from a slurry evaporates, the remaining alkaline chemicals have a greater impact on the solution's pH. With a final pH of 7.8, the slurry seems to have reached a neutral state, making it useful in many agricultural contexts.

Total Solids

The percentage of total solids in the cow dung slurry steadily rises as the slurry is refined. The slurry has a total solids concentration of 15.95% before being dried in the sun. After drying in the sun for 24 hours, this number increases to 20.14%, and after 48 hours, it reaches 22.23%. The final total solids percentage after dewatering is 24.32%. As moisture evaporates during sun-drying and is eliminated during dewatering, the concentration of particles in the slurry becomes more evident. Slurry with a higher total solids' percentage has a higher nutrient content, making it more useful as an organic fertilizer.

Total Kjeldahl Nitrogen

Cow dung slurry's TKN increases gradually as it passes through several phases of processing. Before being dried in the sun, the slurry has a TKN concentration of 0.36%. The TKN rises to 0.39% after 24 hours of sun drying and 0.41% after 48 hours of sun drying. The TKN levels off at 0.42 percent after being dehydrated. The release of nitrogenous substances is caused by microbial activity that occurs during sun-drying. The slurry is a great organic fertilizer for nurturing plant development because of its high TKN content (0.42%).

Available Phosphorus

As slurry goes through the various phases of processing, the concentration of accessible phosphorus always decreases. Before being dried in the sun, the slurry has an initial accessible phosphorus concentration of 81.48 mg/kg. This number decreases to 76.16 mg/kg after 24 hours of sun-drying and to 73.05 mg/kg after 48 hours of sun exposure. Dehydration results in a permanent maintenance of 70.84 mg/kg of accessible phosphorus. Because soluble phosphorus is lost, the amount of accessible phosphorus decreases. Even after being diluted, the slurry still contains a lot of usable phosphorus for further usage.

Available Potassium

As slurry goes through the various steps of processing, the amount of potassium that is still accessible to be used decreases steadily. The initial concentration of accessible potassium in the slurry, prior to sun drying, is 1005 mg/kg. This result drops to 934.33 mg/kg after 48 hours of solar drying, from 958.22 mg/kg immediately after drying. Finally, the available potassium level is maintained at 911.44 mg/kg following dehydration which can be refined into a more concentrated and nutrient-rich form making it a useful resource for farm uses.

Nutrient Concentration Analysis for Liquid form of Output

As the drying and dewatering processes of sun-drying slurry continue, its weight reduces dramatically. However, the fact that the final liquid weight (10.45 kg) is much lower than the starting dry weight (95.44 kg) is crucial in highlighting the large moisture loss during processing. After being dehydrated, the pH level remains stable having dropped gradually during sun-drying. The final liquid product seems to be somewhat less alkaline than the starting slurry (pH 7.6). Here, Sun-drying and dewatering contribute to a notable increase in total solids percentage, highlighting the concentration of solids within the liquid product. The final value of 14.57% indicates a more nutrient-dense product, suitable for enhancing soil fertility and plant growth. The concentration of Total Kjeldahl Nitrogen (TKN) slightly decreases during processing, but the liquid product retains a significant amount (0.31%). While available phosphorus content experiences a minor reduction, the liquid product retains a substantial amount (79.59 mg/kg). Available potassium content also shows a

slight decrease but remains significant (917.10 mg/kg) in the liquid product. The data reveals that the combined sun-drying and dewatering processes effectively reduce the moisture content in cow dung slurry leading to a more concentrated and nutrient-rich liquid product.

5.2.2 Results in terms of Reduction Percentage

The results from analyzing of combined sun-drying and dewatering process of biogas slurry (bio-digestate) by utilizing the same dewatering machine are examined to determine the reduction percentages.

Table 5.5: Results as of Reduction Percentage

Reduction Percentage	Pretreatment (Before Sun-drying)	Pretreatment (After 24 hours of Sun-drying)	Pretreatment (After 48 hours of Sun-drying)	After Dewatering (Solid Form)	After Dewatering (Liquid Form)
Weight (kg)	21.99	21.34	56.02	82.16
pH Value	4.76	1.25	2.50	3.80
Total Solids (%)	-26.27	-10.38	-20.75	34.46
Total Kjeldahl Nitrogen, N (%)	-8.33	-3.85	-7.69	23.46
Available Phosphorus, P (mg/kg)	6.53	4.08	6.99	-8.95
Available Potassium, K (mg/kg)	4.65	2.49	4.88	1.84

Weight

Prior to sun-drying, the slurry's weight has been left unspecified. However, after 24 hours of sun-drying, it exhibits a 21.99% reduction, followed by a substantial 21.34% reduction after sun exposure for 48-hours. The most substantial reduction in weight occurred on dewatering resulting in a significant 56.02% decrease in weight of solid while 82.16% decrease in weight of liquid. The sun-drying and dewatering procedures remove water from the slurry, which is the primary cause of the weight losses. The slurry loses volume and gains density as its moisture content falls.

pH Value

After being exposed to the light for 24 hours, the pH is significantly dropped to 4.76. After 48 hours in the sun, the pH has dropped to 1.25, further highlighting the acidic change. The pH, however, rise somewhat after dewatering, to about 2.50. The buildup of organic acids from microbial activity during sun-drying is responsible for the dramatic decrease in pH. This happens when the slurry is exposed to sunshine. Since the pH rose after being dewatered, it is safe to assume that the solidified slurry is less acidic than the original slurry.

Total Solids

While the initial percentage remains unspecified, after 24 hours of sun-drying, there is a dramatic reduction of 26.27% in total solids. This reduction lessens after 48 hours of sun exposure, resulting in a 10.38% decrease. However, after dewatering, the percentage of total solids saw a notable decrease of 20.75%. These fluctuations in total solids percentage primarily stem from changes in moisture content. The drastic initial reduction during sun-drying reflects the substantial removal of water from the slurry. The final percentage of total solids indicates the denser and more solid nature of the slurry, which is advantageous for storage and handling.

Total Kjeldahl Nitrogen

As the slurry goes through the various phases of processing, the amount of nitrogen in the sample decreased. Before being dried in the sun, the TKN decrease is unknown. Sun-drying for 24 hours resulted in an 8.33% decrease in TKN, and drying for 48 hours resulted in a further 3.85% decrease. Dewatering is the single most important factor in the drastic 7.69% drop in TKN. As water is extracted from a slurry, the nitrogen-containing molecules within

it become more concentrated, leading to a decrease in total soluble nitrogen. Microbial activity during sun-drying may also result in the emission of nitrogenous chemicals.

Available Phosphorus

Slurry samples show both increases and decreases in available-P content after processing. The first available phosphorous content remains undetermined. There is an increase of 6.53 mg/kg after 24 hours of sun-drying, and another rise of 4.08 mg/kg after 48 hours of sun exposure. There is a 6.99 mg/kg uptick after dehydration. The complicated dynamics of phosphorus in the slurry are to blame for such variations in the element's availability. The slurry in its solid state can be a more abundant source of accessible phosphorus, an important nutrient for plant development.

Available Potassium

During the various steps of processing, the concentration of available-K in the slurry varied. There is an increase of 4.65 mg/kg after 24 hours of sun-drying, and another rise of 2.49 mg/kg after 48 hours of sun exposure. Another 4.88 mg/kg rise occurs after dehydration. Concentration shifts of potassium molecules within the slurry presumably play a role in these fluctuations in accessible potassium content. The solidified slurry may be useful as a source of potassium for plant nutrition due to the final rise in accessible potassium concentration.

Reduction Percentage Analysis for Liquid form of Output

Combined Sun-drying and dewatering give important insights into the changes that occur throughout the treatment of slurry sample by comparing the percentage decrease in different parameters. The most substantial reduction occurs after dewatering in the liquid form, with a remarkable 82.16% reduction in weight. The pH value experiences significant reductions after 24 hours of sun-drying (4.76) and further decreases after 48 hours (1.25). However, the pH value slightly increases to 3.80 after dewatering. Total solids percentage shows a remarkable increase of 34.46% after dewatering in liquid form. The total Kjeldahl nitrogen content significantly increases by 23.46% after dewatering in the liquid form. The available phosphorus content experiences fluctuations with a reduction of 8.95% after dewatering in the liquid form. Available potassium content shows a minor increase of

1.84% after dewatering in the liquid form indicating its preservation during processing. Hence, the data demonstrates that the combination of sun-drying and dewatering processes effectively reduces the moisture content in cow dung slurry resulting in a more concentrated or nutrient-rich liquid product for making it a promising alternative to chemical fertilizers and beneficial for soil enrichment and crop growth.

5.2.3 Results from Efficiency Analysis

The performance of the combined sun-drying and dewatering process is evaluated through the assessment of moisture content, dry matter, dewatering efficiency, and dewatering rate for ascertaining the effectiveness of the combined process in achieving desired outcomes.

Table 5.6: Efficiency analysis

Efficiency Measuring Parameters	Pretreatment (Before Sun-drying)	Pretreatment (After 24 hours of Sun-drying)	Pretreatment (After 48 hours of Sun-drying)	After Dewatering (Solid Form)	After Dewatering (Liquid Form)
Weight (kg)	95.44	74.45	58.56	32.74	10.45
Moisture Content, MC (%)	0	22.04	21.40	44.24	68.50
Dry Matter, DM (%)	0	78.01	78.66	55.91	17.84
Dewatering Efficiency, D_E (%)	0	21.99	16.65	27.05	50.41
Dewatering Rate, D_R (%)	0	87.46	33.10	47.81	89.09

The efficiency measuring parameters are assessed at various stages of the process. Initially, before sun-drying, no moisture content is present in the material. After 24 hours of sun-drying, moisture content increases significantly, which continues to decrease after 48 hours. Upon dewatering, the solid form has a lower moisture content compared to the liquid form. Dewatering efficiency shows a steady increase from pretreatment in the form of sun-drying to after dewatering in both solid and liquid forms. Additionally, the dewatering rate displays a notable increase after 24 hours of sun-drying, followed by a decrease after 48 hours. These trends suggest that sun-drying has a substantial impact on reducing moisture content leading to improved dewatering efficiency, particularly after 48 hours of sun exposure followed by the dewatering process using dewatering machine.

5.3 Performance Evaluation of Dewatering Machine

The performance test of existing Dewatering Machine has been conducted at GRIT Engineering Pvt. Ltd. whose results are observed as follow. The weight of solid and liquid extracted along with weight of liquid in cake are examined which are tabulated as follow.

Table 5.7: Performance Results

Test No.	Weight of Feed Sample, W_{fs} (kg)	RPM	Weight of solid cake extracted, W_{ce} (kg)	Weight of Liquid Extracted, W_{le} (kg)	Weight of Liquid in cake, W_{lc} (kg)
1	15	36	7.86	3.26	2.85
2	15	25	7.95	3.07	2.64
3	15	20	8.28	2.96	2.58
4	15	15	8.57	2.85	2.42
5	15	10	8.72	2.76	2.26
6	15	8	8.9	2.55	1.95

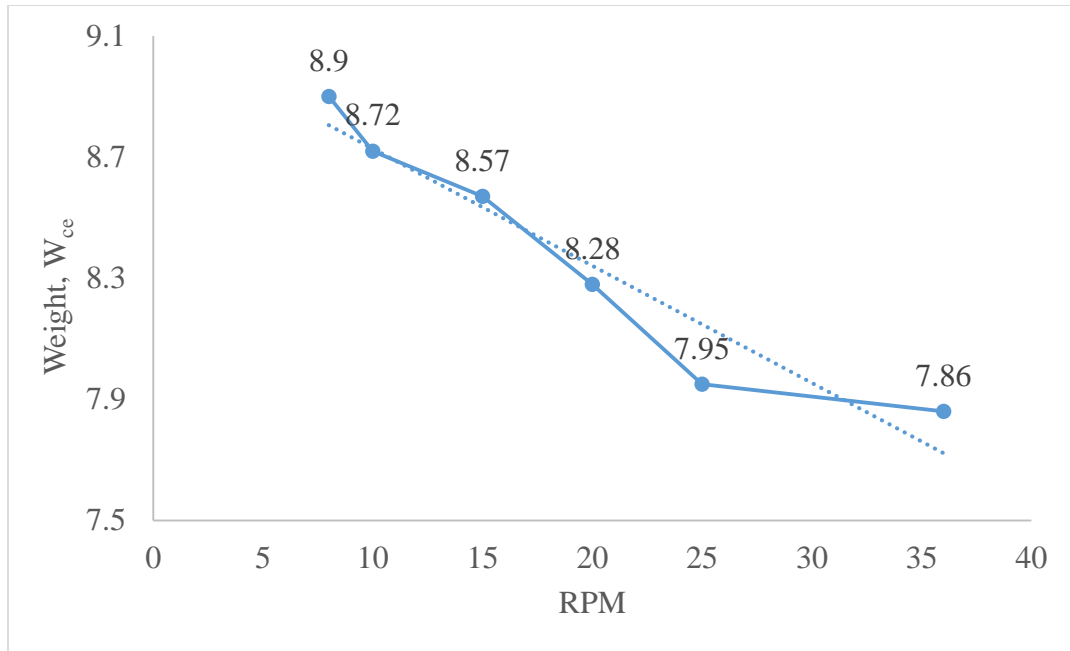


Figure 5.1: RPM vs. Weight of solid cake extracted

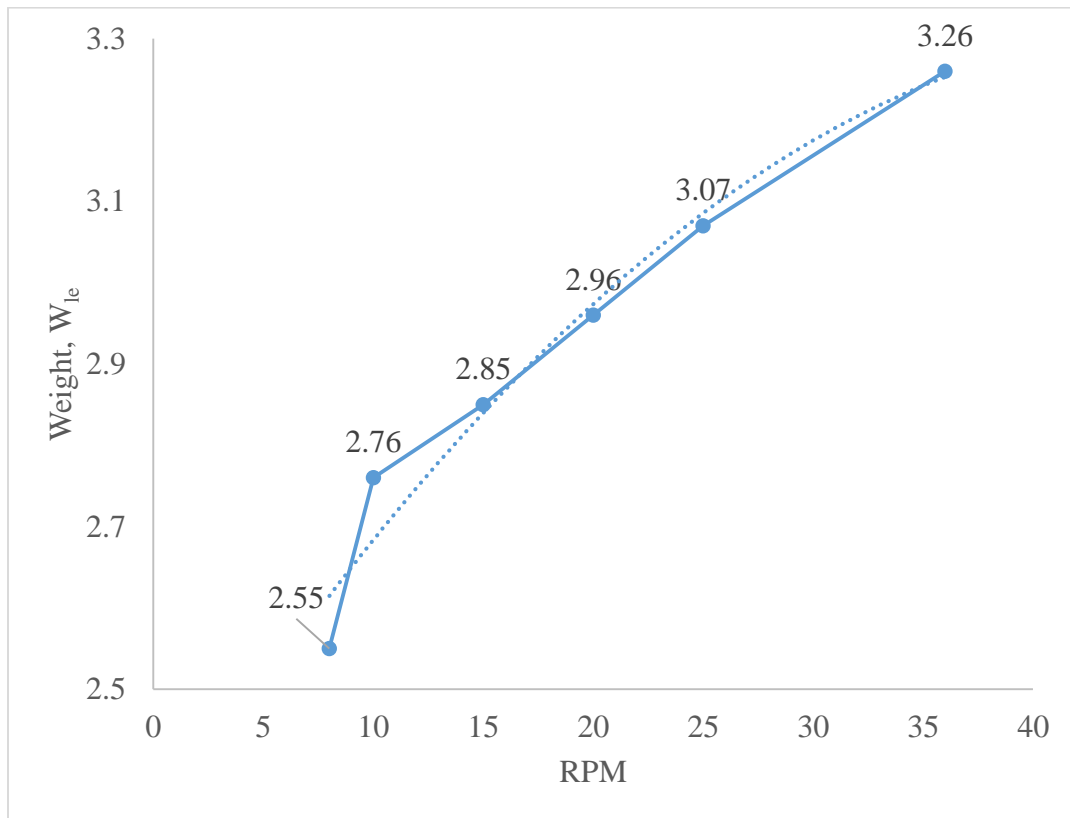


Figure 5.2: RPM vs. Weight of Liquid Extracted

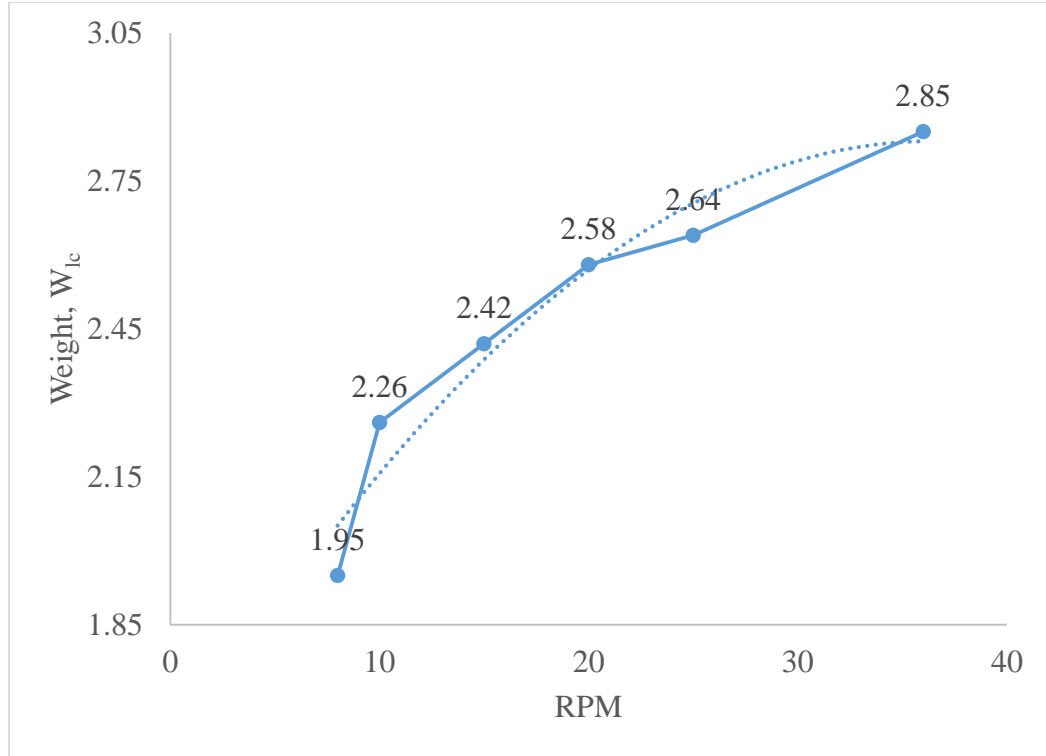


Figure 5.3: RPM vs. Weight of Liquid in cake

The biogas slurry samples, after undergoing a pre-treatment process of sun-drying for 24 hours, have been subjected to dewatering, with an initial weight of 15 kg consistently maintained for feeding at machine. As the RPM settings decrease from 36 to 8, several key trends emerge. The weight of solid cake extracted (W_{ce}) increases progressively, reaching 8.9 kg at 8 RPM. This signifies that lower RPM settings contribute to more efficient solid cake extraction. Conversely, the weight of liquid extracted (W_{le}) decreases with decreasing RPM, indicating that higher RPM settings result in a greater amount of liquid being extracted. Moreover, the weight of liquid in the cake (W_{lc}) also exhibits a downward trend as RPM decreases, suggesting that lower RPM settings are favorable to producing drier cakes. In summary, the data demonstrates that reducing the RPM setting on the dewatering machine enhances its performance in terms of solid cake extraction and minimizing the presence of liquid in the cake. These findings are valuable for optimizing dewatering processes for pre-treated biogas slurry samples potentially improving efficiency and product quality.

Table 5.8: Results on Yield, Extraction Efficiency and Loss

Test No.	RPM	Extraction Yield, E_y (%)	Extraction Efficiency, E_e (%)	Extraction Loss, E_l (%)
1	36	44.03	69.87	25.87
2	25	45.07	70.67	25.73
3	20	47.10	73.60	25.07
4	15	49.20	76.18	23.87
5	10	50.52	77.51	23.47
6	8	52.51	79.11	22.80

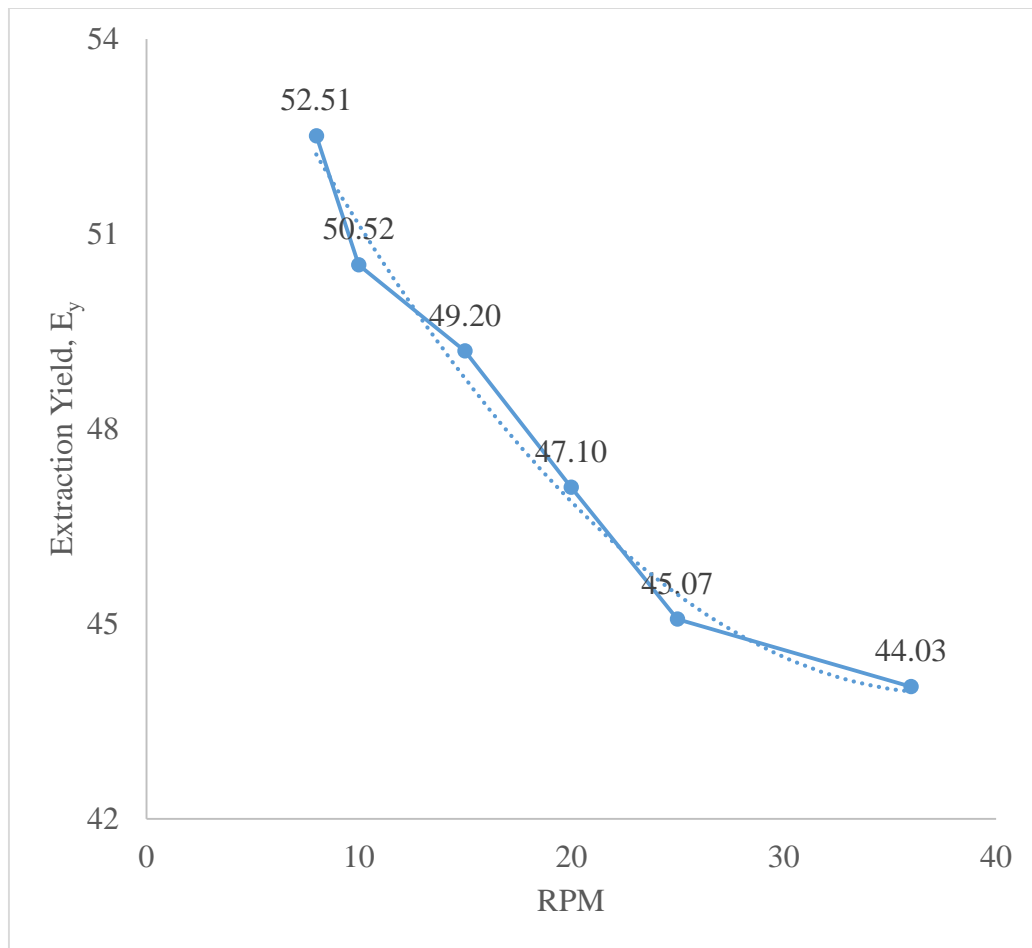


Figure 5.4: Graph on RPM vs. Extraction Yield

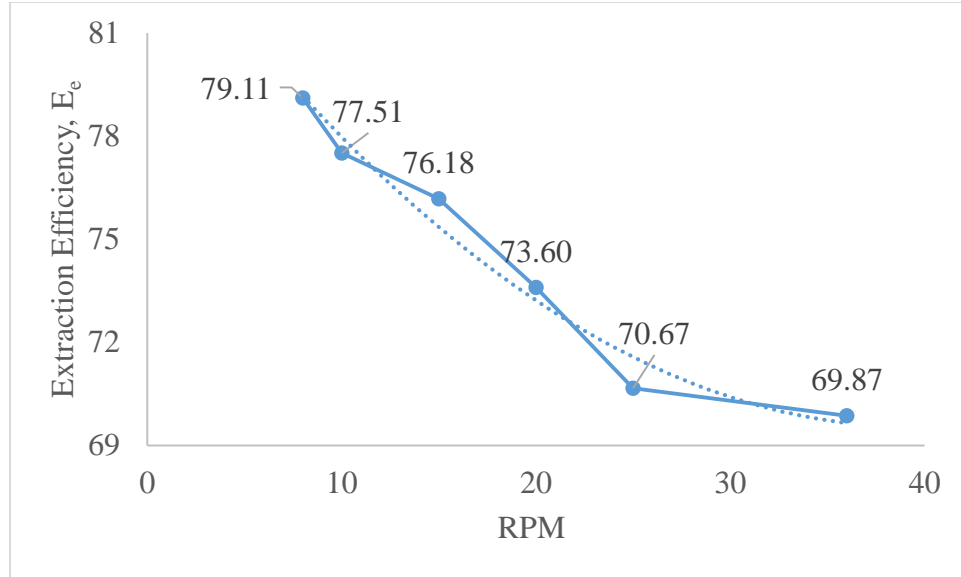


Figure 5.5: Graph on RPM vs. Extraction Efficiency

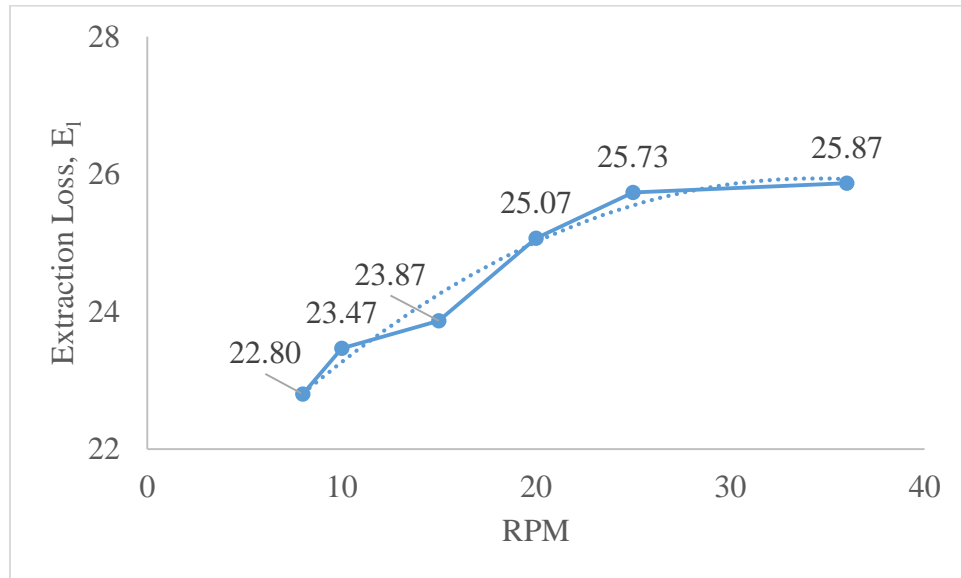


Figure 5.6: Graph on RPM vs. Extraction Loss

In case of dewatering machine with varying RPM settings, the focus is on extraction-yield, extraction-efficiency and extraction-loss without including MC. As the RPM decreases from 36 to 8, several noteworthy trends become evident. Extraction yield consistently increases with decreasing RPM, rising from 44.03% at 36 RPM to 52.51% at 8 RPM. This indicates that lower RPM settings result in higher extraction yields. Extraction efficiency also exhibits a consistent upward trend, increasing from 69.87% to 79.11% as RPM

decreases. This highlights that lower RPM settings contribute to greater extraction efficiency, allowing more efficient separation of solid cake from liquid. Conversely, extraction loss decreases as RPM decreases, dropping from 25.87% at 36 RPM to 22.80% at 8 RPM, signifying that lower RPM settings are associated with reduced extraction loss. In summary, the data suggests that lowering the RPM setting on the dewatering machine when processing pre-treated biogas slurry samples leads to improved extraction yield, efficiency and reduced extraction loss. These findings are valuable for optimizing dewatering processes potentially increasing overall efficiency and minimizing product loss.

5.4 Comparative Analysis

A comparative analysis is conducted on the results obtained from both the sun-drying process and the combined sun-drying and dewatering process. This assessment aims to identify differences and similarities in outcomes facilitating a comprehensive understanding of their respective effectiveness and performance.

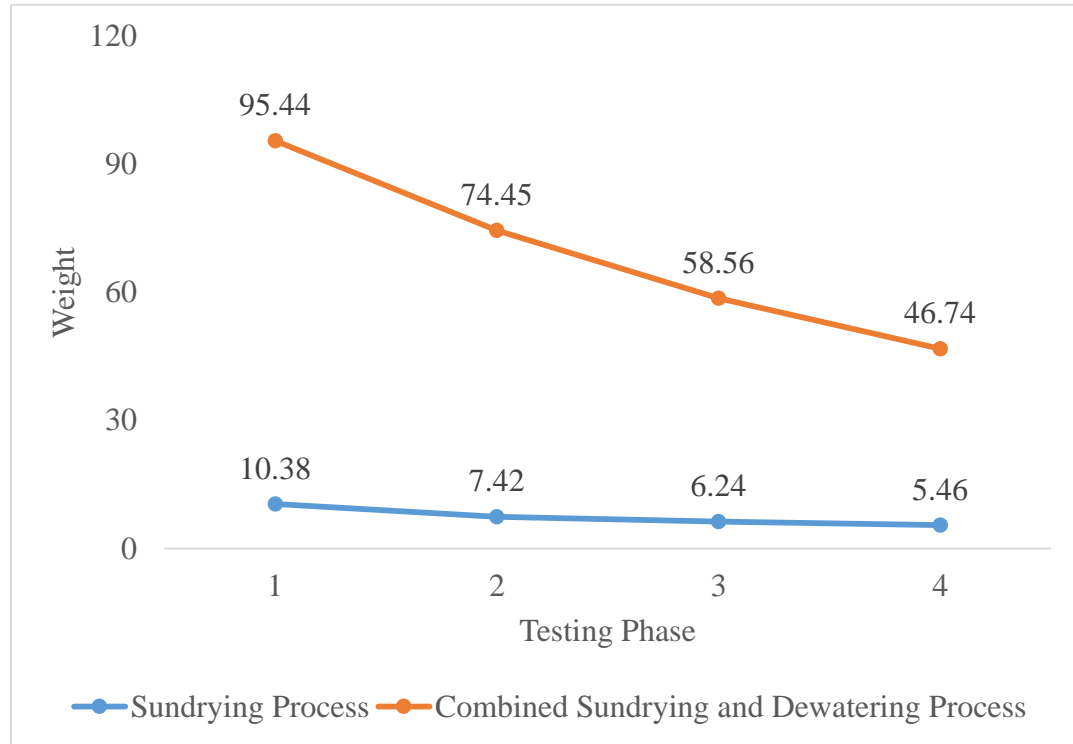


Figure 5.7: Weight Comparison

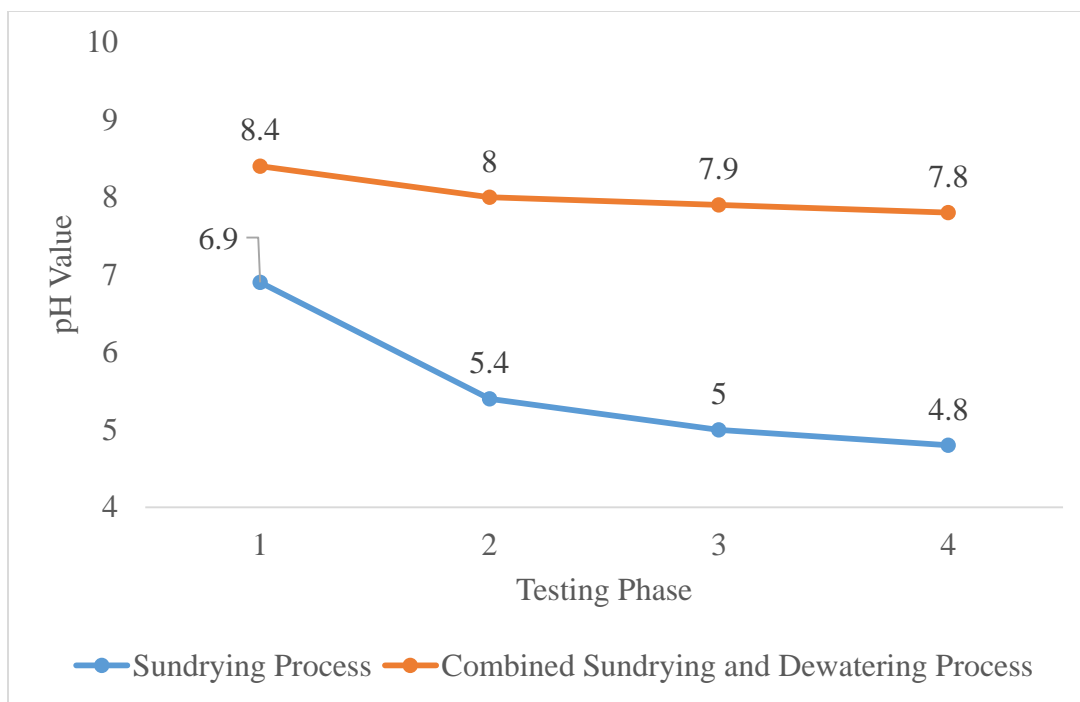


Figure 5.8: pH Value Comparison

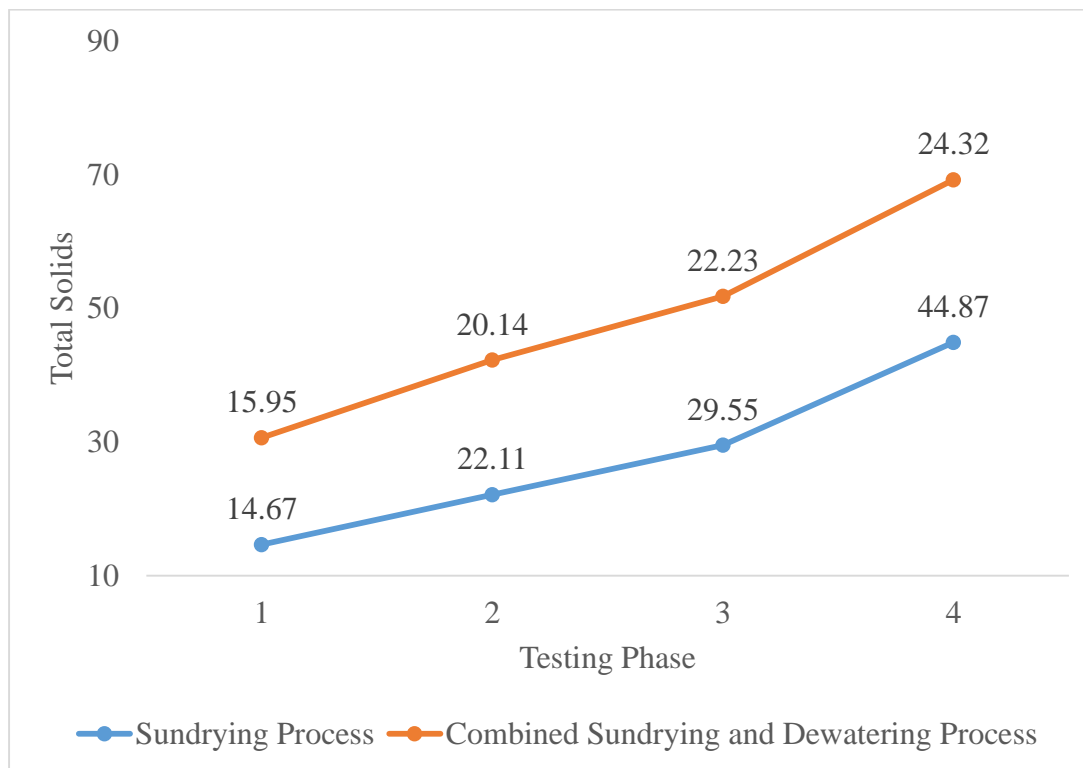


Figure 5.9: Total Solids Comparison

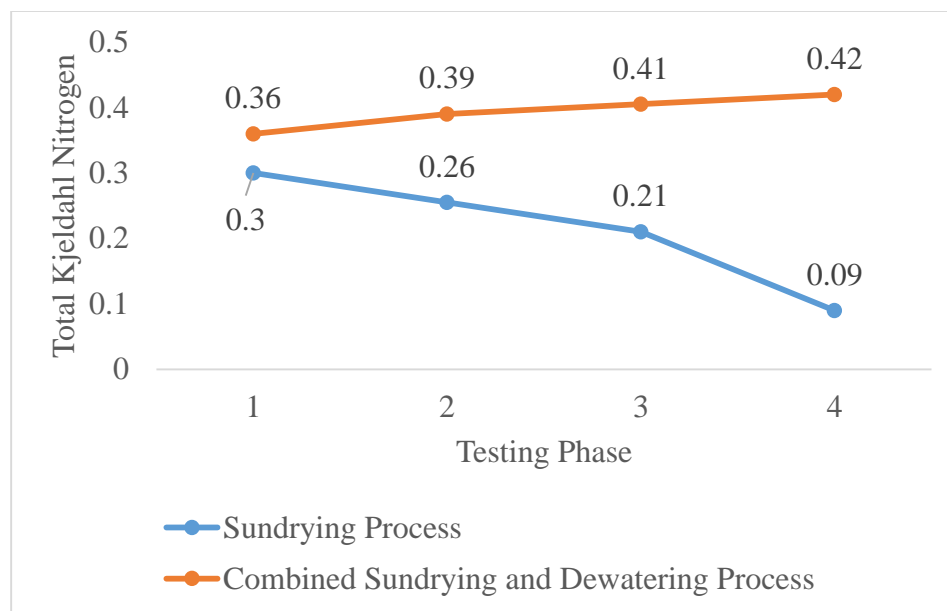


Figure 5.10: Total Kjeldahl Nitrogen Comparison

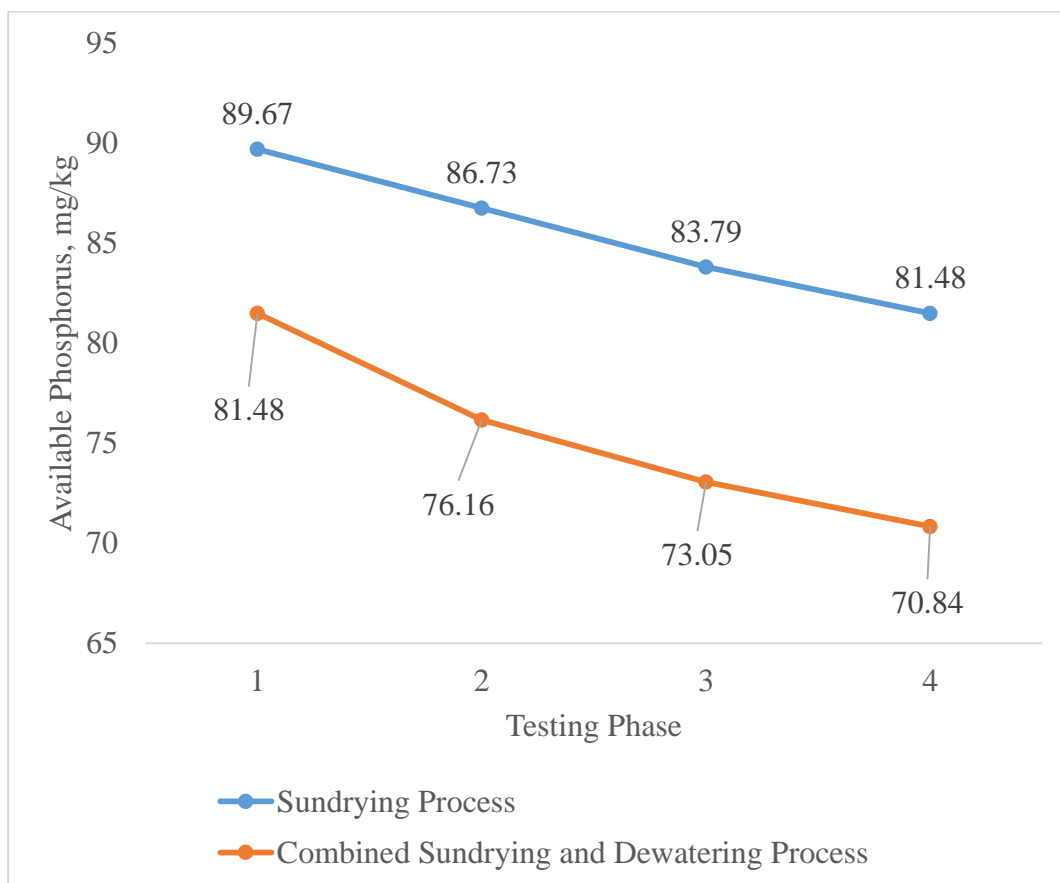


Figure 5.11: Available Phosphorus Comparison

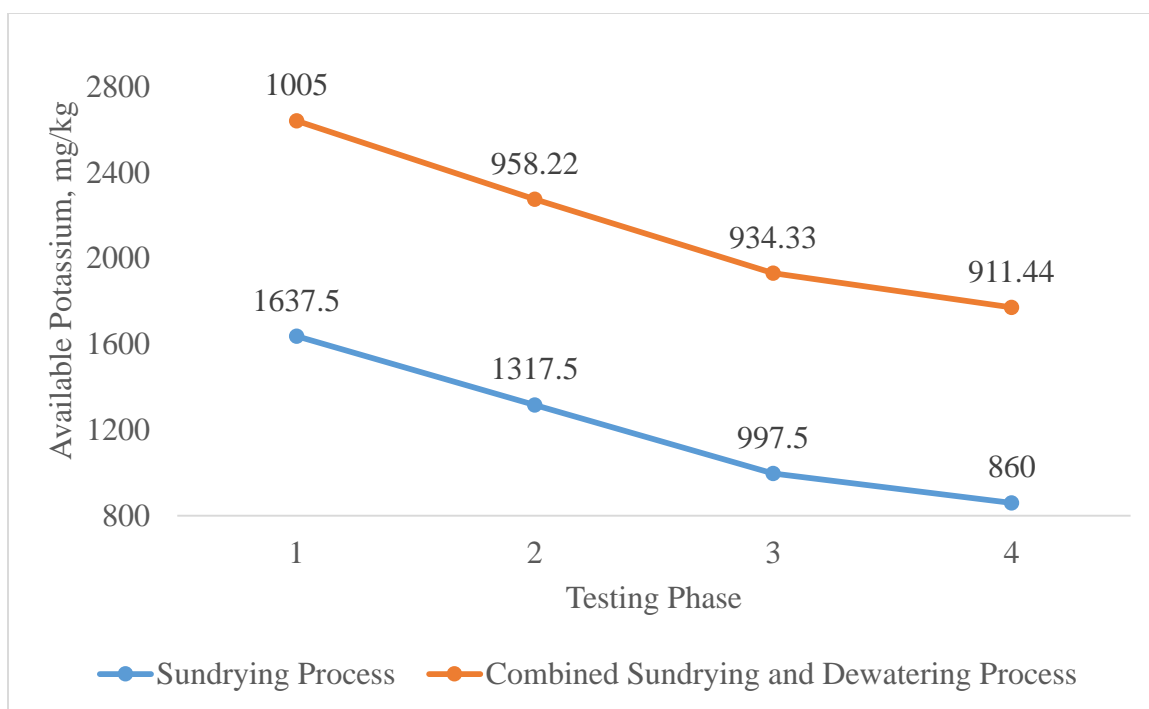


Figure 5.12: Available Potassium Comparison

The comparative analysis reveals that the combined sun-drying and dewatering method outperforms sun-drying alone in achieving moisture reduction and solid concentration in cow dung slurry. This approach offers advantages in pH control and stability making it the preferred choice for processing cow dung slurry for various agricultural applications. Additionally, it is the most effective method for increasing the Total Kjeldahl Nitrogen (TKN) content, enhancing its suitability as an organic fertilizer. While it reduces available phosphorus, it remains valuable as a nutrient source for plant growth. The combined sun-drying and dewatering method emerges as the optimal strategy for maximizing the nutritional content and agricultural suitability of cow dung slurry.

Table 5.9: Comparison of solid form of slurry with compost

Nutrient Contents	Nitrogen, N (%)	Phosphorus, P (%)	Potassium, K (%)
Average Home-Made Compost	0.5	0.27	0.81
From present study (Maximum Value)	0.42	0.01	0.125

Table 5.10: Comparison of liquid form of slurry with comfrey liquid

Nutrient Contents	Nitrogen, N (%)	Phosphorus, P (%)	Potassium, K (%)
Comfrey Liquid	0.014	0.0059	0.0340
From present study (Liquid Form)	0.31	0.01	0.0917

(Composts & Fertilisers , 2023)

The results obtained show that the nutrient content in the cow dung biogas slurry sample used in the study are almost near to standard value of the reviewed data of cow dung manure available in the market in case of solid form of sample but the liquid form extended the nutrient content than the comfrey liquid.

Comparing with DAP and Urea

DAP (18-46-0), indicating 18% Nitrogen (N), 46% Phosphorus (P_2O_5), and 0% Potassium (K_2O). While, Urea contains approximately 46% Nitrogen (N). Urea has a nitrogen content of about 46%, which is substantially higher than the TKN percentages in the sundried and dewatered samples. DAP has around 18% nitrogen, which is also higher compared to the sample. Also, the DAP has a phosphorus content of about 46% (as P_2O_5). The sample, even before any treatment, has significantly less phosphorus. Similarly, DAP doesn't typically contain potassium. However, the sample has a significant amount of potassium, especially before sun-drying.

The sample, after sun-drying and dewatering contains lower amounts of TKN (N) and Phosphorus compared to standard fertilizers like DAP and Urea. Potassium levels in the sample are significant making it potentially a good source of potassium. This analysis provides an opportunity to understand the change of nutrient composition of organic materials during sun-drying and dewatering process. While, the sample with its potassium content can be blended with other fertilizers or materials to enhance its overall nutrient value.

Efficiency Loss Analysis

The efficiency analysis is performed with a focus on Separation Efficiency (Se) and Nutrient Loss Efficiency (NLe) to assess the effectiveness of slurry samples in terms of their ability to separate components and minimize nutrient loss in the process of research.

Table 5.11: Results from Efficiency Analysis

Efficiency Analysis	Sun-drying Process	Combined Sun-drying and Dewatering Process
Separation Efficiency (Se)	67.3055	34.4161
Nutrient Loss Efficiency (NLe) for N	70	-16.667
Nutrient Loss Efficiency (NLe) for P	9.13349	13.0584
Nutrient Loss Efficiency (NLe) for K	47.4809	9.30945

In terms of separation efficiency, the sun-drying process significantly outperforms the dewatering process with a Se of approximately 67.3% compared to 34.4%. The sun-drying process exhibits higher NLe for N (70%) compared to the dewatering process (-16.7%). This implies that the sun-drying process retains more nitrogen nutrients, which can be advantageous for nutrient preservation. On the other hand, for phosphorus (P) and potassium (K), the dewatering process shows better NLe values (P: 13.1%, K: 9.3%) than the sun-drying process (P: 9.1%, K: 47.5%). In conclusion, while sun-drying excels in separation efficiency and nitrogen preservation, the combined sun-drying and dewatering process appears to be more efficient in retaining phosphorus and potassium nutrients.

5.5 Time and cost efficiency Analysis

The efficiency analysis, specifically pertaining to time and cost efficiency consist of calculations as part of research to evaluate and quantify the efficiency of both the studied process in terms of both time utilization and cost effectiveness as follow.

a.) Time Efficiency = (Time saved with dewatering ÷ Total time for sun-drying) × 100

$$= [(72 - (48+4)) \div 72] \times 100 = 27.78\%$$

b.) Cost Efficiency = (Cost saved with dewatering ÷ Cost of sun-drying) × 100

Where, Cost saved with dewatering = Cost of sun-drying - Cost of dewatering

And, Cost of sun-drying = 12,000 (land on rent per month) + 20,500 (labor cost per month) + 165,500 (Loss of Cost due to selling the manure with reduced nutrient content) = NRs. 197,500

Cost of dewatering = 3266 (Maintenance Cost per month) + 13,898 (operating cost per month) + 61,500 (labor cost) + 3266 (Interest paid for loan per month) + 32,666 (Investment cost per month) = NRs. 114,596

So, Cost Efficiency = (82,904 ÷ 197,500) × 100 = 42%

c.) Cost Efficiency Ratio (Sun-drying) = 197,500 ÷ 86.89 = 2272.989

d.) Cost Efficiency Ratio (Dewatering) = 114,596 ÷ 50.91 = 2250.953

Combined sun-drying and dewatering can significantly reduce the time required for the drying process, which can be particularly beneficial in situations where time is a critical factor. Combined sun-drying and dewatering is a more cost-effective method when considering the overall expenses involved in both processes, resulting in substantial cost savings. The combined sun-drying and dewatering process is slightly more favorable in terms of cost efficiency along with cost efficiency ratio. Comparative analysis suggests that combined sun-drying and dewatering is a promising alternative to traditional sun-drying for the drying of certain materials. It not only offers time savings but also proves to be more cost-efficient, making it a viable option for industries or processes where these factors are crucial.

CHAPTER SIX: FINANCIAL ANALYSIS RESULTS AND DISCUSSIONS

6.1 Financial Analysis

For the dewatering equipment, the user has to incur a cost of NRs. 392,000. The operation and packaging of fertilizer after complete dewatering of product need the involvement of three laborers. Assuming a monthly compensation of NRs. 20,500, inclusive of salary with benefits, the total yearly labor cost amounts to NRs. 738,000.

Assuming that the dewatering machine can be run for a total of 300 days per year.

The operational expenses of the dewatering machine include (5Hp) of motor and (1Hp) of slurry pump. The machine runs for a duration of 10-hours every day. Subsequently, the monetary value associated with the use of power amounts to NRs. $(10 \times 6 \times 0.7457 \times 12.50 \times 300 = 166,770)$. The yearly maintenance cost of the dewatering machine is estimated to be 10% of the overall cost. So, annual maintenance expense amounts to NRs. 39,200.

Table 6.1: Annual Cash Flow

S. No.	Particulars of Cash Flow (Annual)	Amount (NRs)
1.	Initial Cost	3,92,000
2.	Operating Cost	1,66,770
3.	Labor Cost	7,38,000
4.	Maintenance Cost	39,200
5.	Interest Paid to Donor @10% annually	39,200
6.	Income	11,90,000

1. Initial Cost = NRs. 384000 + NRs. 8000 (Cost of assembly and testing) = NRs. 392000
2. Annual Operating cost = Cost of electricity usage (Motor: 5hp; Slurry pump: 1hp; Machine operated: 10 hrs. a day) = $10 \times 6 \times 0.7457 \times 12.50$ (NRs.) = NRs. 555.9 per day = NRs. 166770 (Assuming 300 days of operating the machine).
3. Annual Labor Cost: (Assuming the monthly salary of one labor as NRs. 20500 and in total three labors are required in operation) = $3 \times 12 \times 20500$ = NRs. 738000
4. Annual Maintenance Cost = 10% of initial cost = NRs. 39200
5. Annual Simple Interest Paid to Donor = 10% of initial cost = NRs. 39200
6. Annual Income:

Considering biogas plant of 1m^3 , then output of plant: 1000 kg/day.

Performance ratio by weight is 7, so output: 173 kg per day.

With 70% as efficiency; output per day is 100 kg per day.

Market value of per kg of organic fertilizer = NRs. 35 (Assuming $365 - 25 = 340$ days of active production)

Hence, annual income = NRs. 11,90,000

6.2 Payback Period

It denotes number of years needed to get back the initial investment.

Annual Income = 11,90,000

Annual Expenses = Operating cost + Labor cost + Maintenance cost + Annual interest paid

$$= 166770 + 738000 + 39200 + 39200$$

$$= \text{NRs. } 983170$$

Now, Net Annual Profit = Annual Income – Annual Expenses

$$= 1190000 - 983170$$

$$= \text{NRs. } 206830$$

$$\begin{aligned}
\text{Therefore, Payback period} &= \frac{\text{Total Investment (Initial)}}{\text{Annual Profit}} \\
&= \frac{392000}{206830} = 1.895276314 \text{ years} = 692.2354608 \text{ days} \\
&= 1 \text{ year } 10 \text{ months } 23 \text{ days}
\end{aligned}$$

The repayment duration in this research is computed as 1 year 10 months and 23 days, which is less than the payback period in *Sherpa et al.'s 2017* study. This is because a lower price is selected as NRs. 35 rather than NRs. 50 in previous study, which is closer to the real market price for the fertilizer extracted from the dry cake. The overall machine cost in our analysis is NRs 392,000, which is a little more than the NRs 350,000 in *Sherpa et al.'s* study. The usage of a 5HP motor with a reduction gear system, as opposed to their 1HP motor, and the modification of worker salaries on a monthly basis rather than daily salary along with operating cost increment are credited for this difference.

6.3 Internal Rate of Return

Let us consider a hypothetical scenario in which the equipment operates for a duration of five years, after which it needs a full replacement.

And, when this discount rate is applied, the NPV of a business project's cash flows is zero. The rate of profit retained by the business is known as IRR.

Here,

Using excel command; IRR = IRR (-392000, 376830, 376830, 376830, 376830, 376830)

i.e., IRR = 44 %

It has been determined that the dewatering machine has IRR of 44%. It is taken as a financial measure for evaluating the profitability of project. An IRR of 44% means that the investment is estimated to produce a return of 44% on the initial capital invested over a specified time period.

6.4 Net Present Value

The NPV is a financial measure used to determine the PV of a dewatering machine. Given an assumed duration of 5 years.

So, Using excel command; NPV = NPV (-392000, 376830, 376830, 376830, 376830, 376830) @10% interest per annum

i.e., NPV = NRs. 353575.86

The net present value is calculated as Nepalese Rupees Three lakh fifty-three thousand Five hundred seventy-five rupees and Eighty-six paisa.

CHAPTER SEVEN: CONCLUSIONS AND RECOMMENDATIONS

7.1 Conclusions

The project's conclusions are derived from the accomplished work of design, simulation and testing the machine. Such conclusions are:

- i. Based on static structural results, it is evident that the Constant pitch screw with a tapered shaft experiences the lowest stress of 43.941 MPa and strain of 0.00022607 mm/mm compared to other screw types.
- ii. In terms of Computational Fluid Dynamics (CFD) results, the screw press configuration having Constant pitch screw with a tapered shaft, exhibits the highest-pressure difference of 90.165 and turbulence kinetic energy as $1.907e-003 \text{ m}^2/\text{s}^2$. So, the use of a tapered shaft with a screw of constant pitch proves to be the most reliable and effective choice for designing and fabricating the pressing screw for the system.
- iii. The relationship between rotational speed (RPM) and machine performance is evident with lower value i.e., 8 RPM resulting in increased liquid extraction efficiency and lower extraction loss improving overall efficiency of the system.
- iv. From sun-drying of slurry for durations of 24, 48 and 72 hours, the optimal duration is considered as of 48hours of sun-drying due to least Total Solids reduction percentage i.e., -33.65. In terms of nutrient recovery, the combined sun-drying and dewatering process is obtained as better while the time and cost efficiency of it is also greater with 27.78% and 42% respectively in case of efficiency comparison.
- v. According to the financial assessment, the initial cost for installing the machine amounts to NRs 392,000. The analysis determines that the payback period can be achieved in 1 year, 10 months, and 23 days. Additionally, IRR is calculated as 44%, and NPV is found to be NRs. 3,53,575.86.
- vi. The combined form of Sun-drying and dewatering process contributes to the concentration and stabilization of biogas slurry increasing its storage stability and nutritional content which is essential for various applications. The project also includes the packaging of the final dried fertilizer product, ready for distribution to

the market thereby providing a comprehensive solution for the management and utilization of biogas digestate.

- vii. Approximately 28.51% of the slurry sample in solid form and 71.48% in liquid form at initial stage, undergoes sun-drying for up to 72 hours resulting in a final composition of 12.5% solid and 87.5% liquid. However, to achieve the optimal dried sample may require an additional 5 days and 10 hours totaling about 130 hours of sun-drying.
- viii. In a combined process involving sun-drying and dewatering lasting 52 hours, around 21.99% of the solid part and 78% of the liquid part at its initial stage of sampling reach a composition of 20.18% solid and 79.81% liquid. To obtain the optimum dried sample, an extra 13 hours of sun-drying making a total of 61 hours from initial phase may be necessary including the pretreatment process. Hence, the combined process reaches a composition close to the desired level in a shorter overall time frame (61 hours) compared to the prolonged sun-drying process (130 hours) in terms of weight.

7.2 Recommendations

Drawing from the expertise in design, simulation and performance evaluation, the following factors are suggested for recommendations.

- Manufacturing a screw with a tapered shaft and constant pitch is challenging due to the precision required in its orientation and shape.
- To extract a higher amount of nutrient content from a slurry sample for sun-drying followed by the dewatering process, it is important to collect the sample within 10 days from the plant where slurry is formed after the biogas production.
- For biogas slurry samples, initial thickening of samples should be achieved using advanced technologies such as Gravity thickener or clarifier. Subsequently, the sun-drying process coupled with a screw press dewatering system should be employed.
- The blending of biogas slurry sample with urea for Nitrogen boost, DAP for Phosphorus boost, and Potash fertilizer for additional Potassium shall be adhered for optimized content of nutrients (N, P, K) in the slurry sample.

REFERENCES

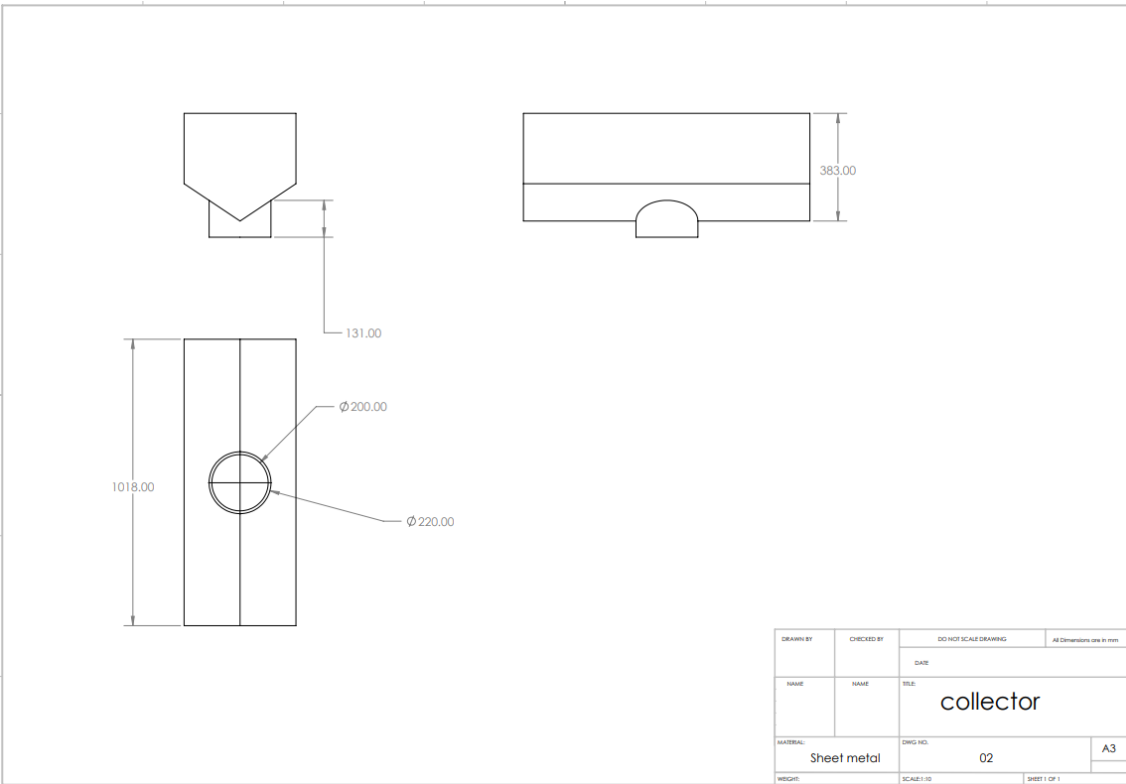
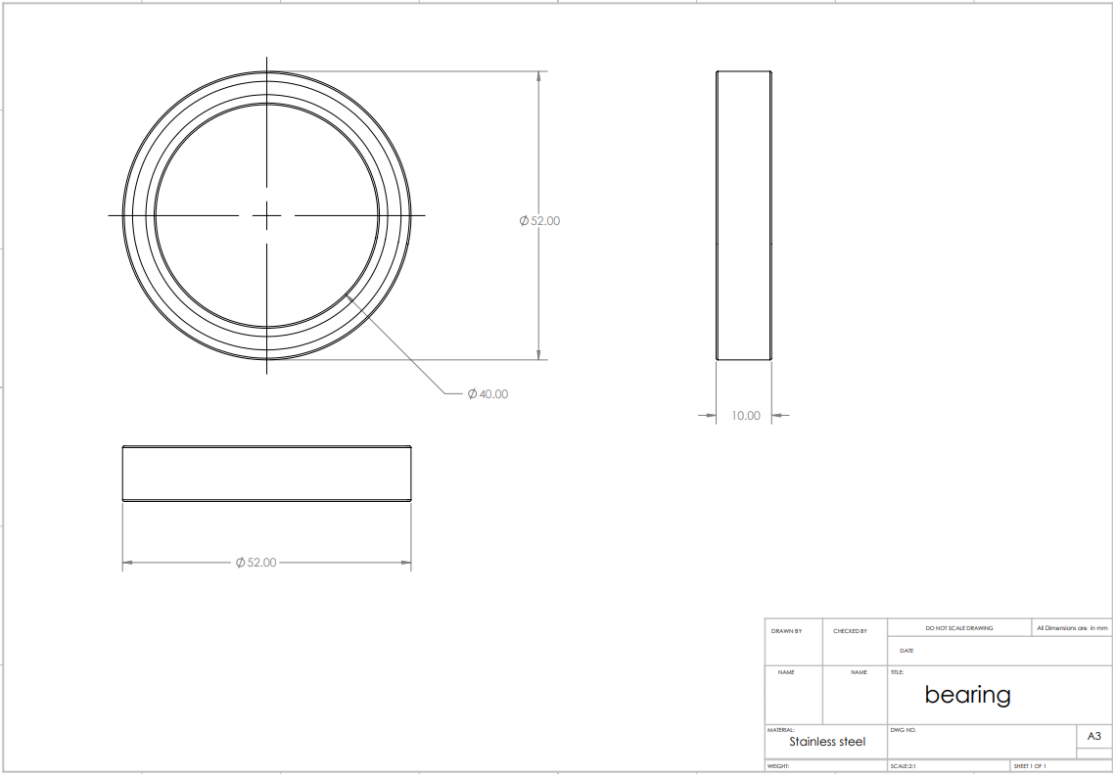
- I. Nawi, Z. Ngali, M. Firdaus, S.M. Salleh, E.M. Yusup & W.A. Siswanto . (2017). Preliminary Design on Screw Press Model of Palm Oil Extraction Machine. *IOP Conf. Series: Materials Science and Engineering*. IOP Publishing.
- AEPC. (2021). *Progress At Glance: A Year In Review FY 2077/78 (2020/21)*. Alternative Energy Promotion Centre.
- Arora K. & Sharma S. (2016). Review on Dehydration and Various Applications of Biogas Slurry for Environmental and Soil Health. *Journal of Rural Development*, 35(1), 131–152. Retrieved from <https://nirdprojms.in/index.php/jrd/article/view/91611>
- Bernhard Drosch et. al. (2015). *Nutrient Recovery by Biogas Digestate Processing*. UK: IEA Bioenergy.
- Bhat A. (2023). *CFD applied to decanter centrifuges*. SWEDEN: CHALMERS UNIVERSITY OF TECHNOLOGY.
- Chitte P. G., Tapsi P. & Deshmukh B. B. (2022.). Design and Development of Dewatering Screw Press. *Recent Advances in Manufacturing Modelling and Optimization* (pp. 569-578). Singapore: Proceedings of RAM 2021.
- Chutimanukul P., Iad-ak R. and Thepsilvisut O. (2023). The Effects of Shading and Nutrient Management on Yield Quality of Vegetable Fern. *Horticulturae*, 9(2), 259.
- Composts & Fertilisers* . (2023). Retrieved from Allotment & Gardens: <https://www.allotment-garden.org/composts-fertilisers/npk-nutritional-values-animal-manures-compost/>
- Emerging Technologies for Biosolids Management*. (2006, September). Retrieved from EPA.gov: <https://www.epa.gov/biosolids/emerging-technologies-biosolids-management>

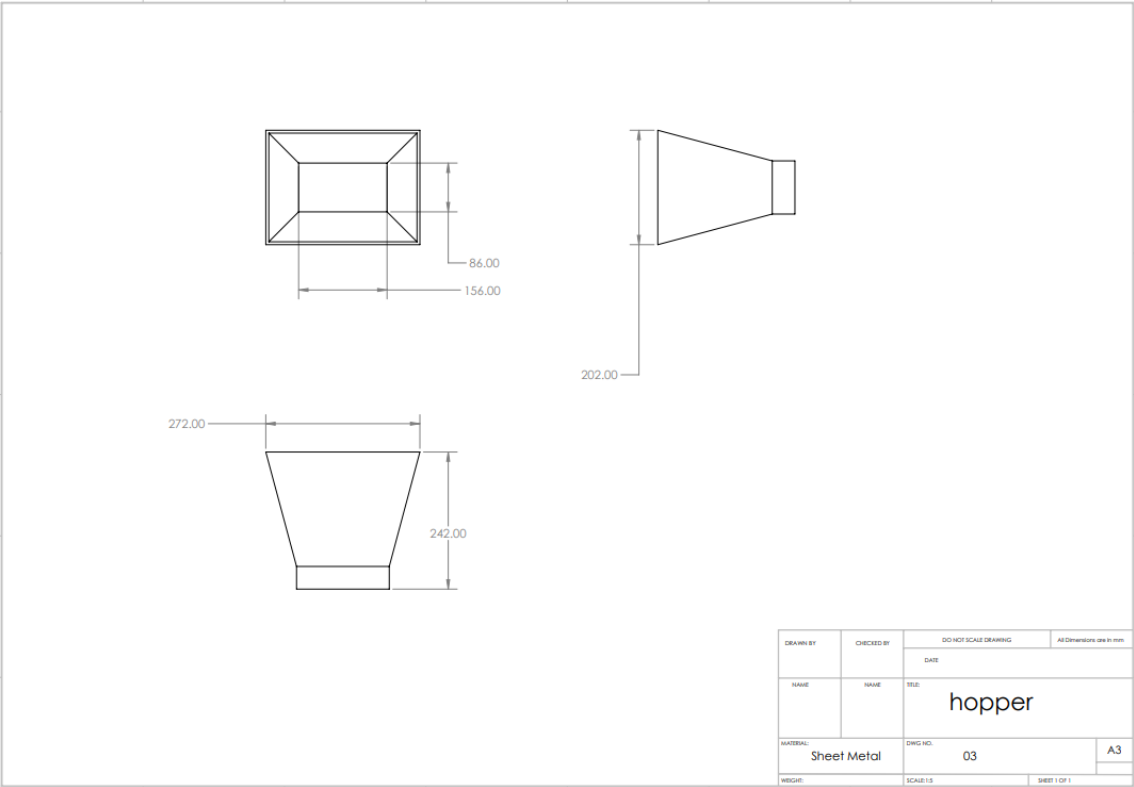
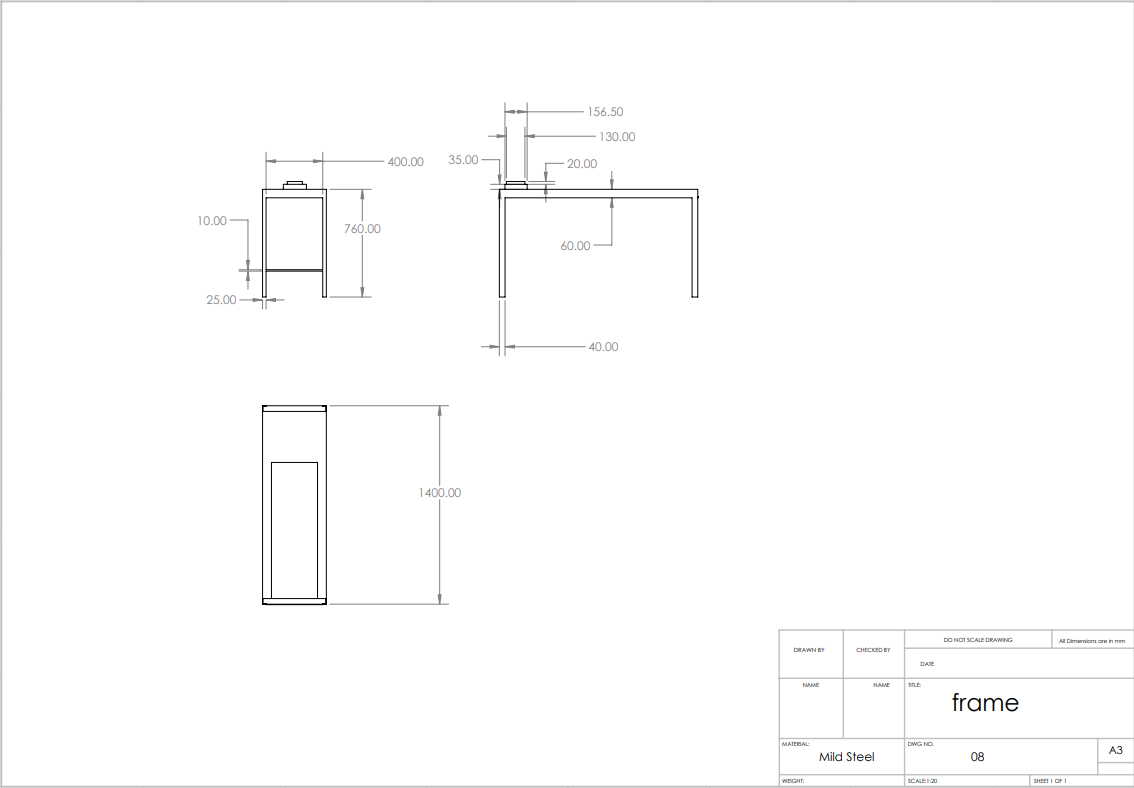
- Er R. Kadam, Dr. D. Sharma and Er. A. Pawar. (2017). Filtration of biogas spent slurry and it's chemical analysis. *International Journal of Chemical Studies*, 5(3), 405-408.
- Er. Rahul Kadam, Dr. Deepak Sharma & Er. Ashish Pawar. (2017). Filtration of biogas spent slurry and it's chemical analysis. *International Journal of Chemical Studies*; 5(3), 405-408.
- Fu S., Dou B., Zhang X. & Li K. (2023). An Interactive Analysis of Influencing Factors on the Separation Performance of the Screw Press. *Separations*, 245.
- Goss C. T., Alsanea A., West J., Barry M., & Marx J. (2019). Balancing Operator Input and Cost: A Case Study for Dewatering Technology Selection. *WEFTEC 2019*. Water Environment Federation.
- Hussein Y. A., Alenyorege E. A. & Adongo T. A. (2015). Extraction Yield, Efficiency And Loss Of The Traditional Hot Water Floatation (HWF) Method Of Oil Extraction From The Seeds Of *Allanblackia Floribunda*. *International Journal of Scientific & Technology Research, Volume 4, Issue 02*,.
- J.K., Khurmi R.S. & Gupta. (2005). *A textbook of machine design*. S. Chand publishing.
- John K. Bernard. (2016). *Measuring the Dry Matter Content of Feeds*. University of Georgia.
- Karki A. B. (2006). *Country Report on the Use of Bio-Slurry in Nepal*.
- L. Morey, B. Fernández et. al. (2023). Acidification and solar drying of manure-based digestate to produce improved fertilizing products. *Journal of Environmental Management, Volume 336*.
- M. Ford and R. Fleming. (2002). *Mechanical Solid-Liquid Separation of Livestock Manure Literature Review*. Ontario: Ridgetown College - University of Guelph.
- M. More, C. Agrawal and D. Sharma. (2023). *Development of Screw Press-Dewatering Unit for Biogas Slurry*. Rajasthan, India: Researchgate.

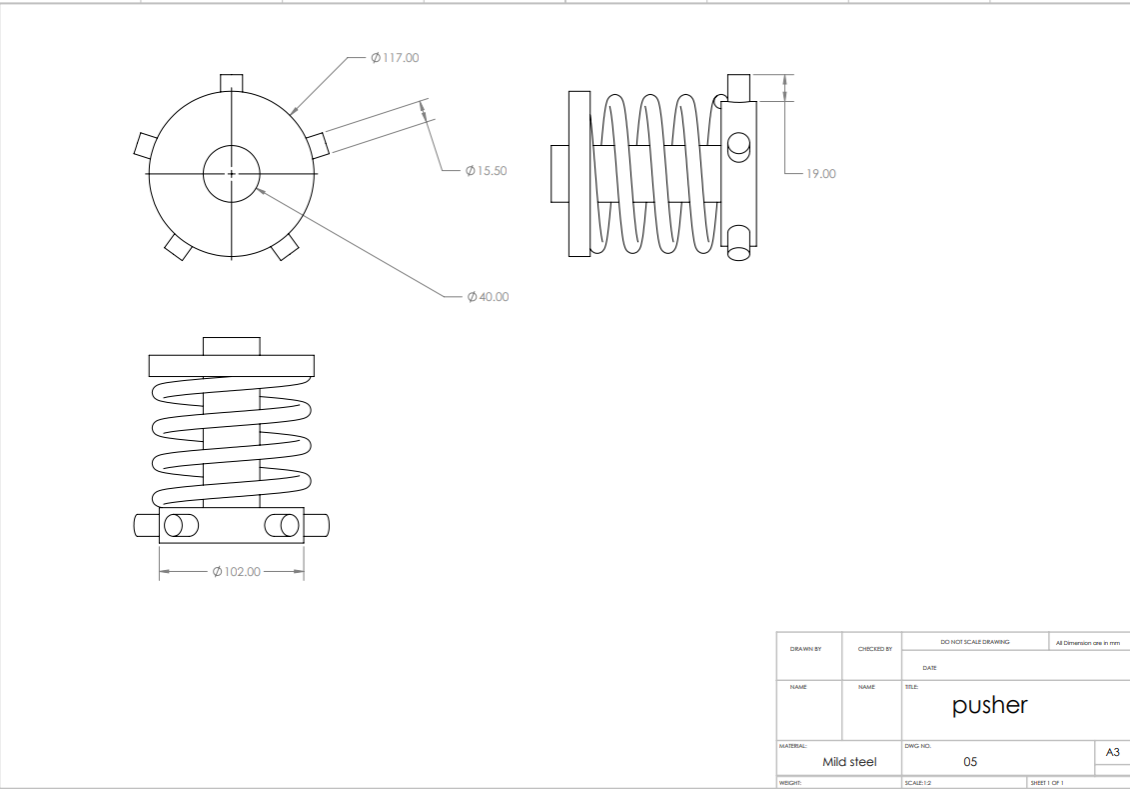
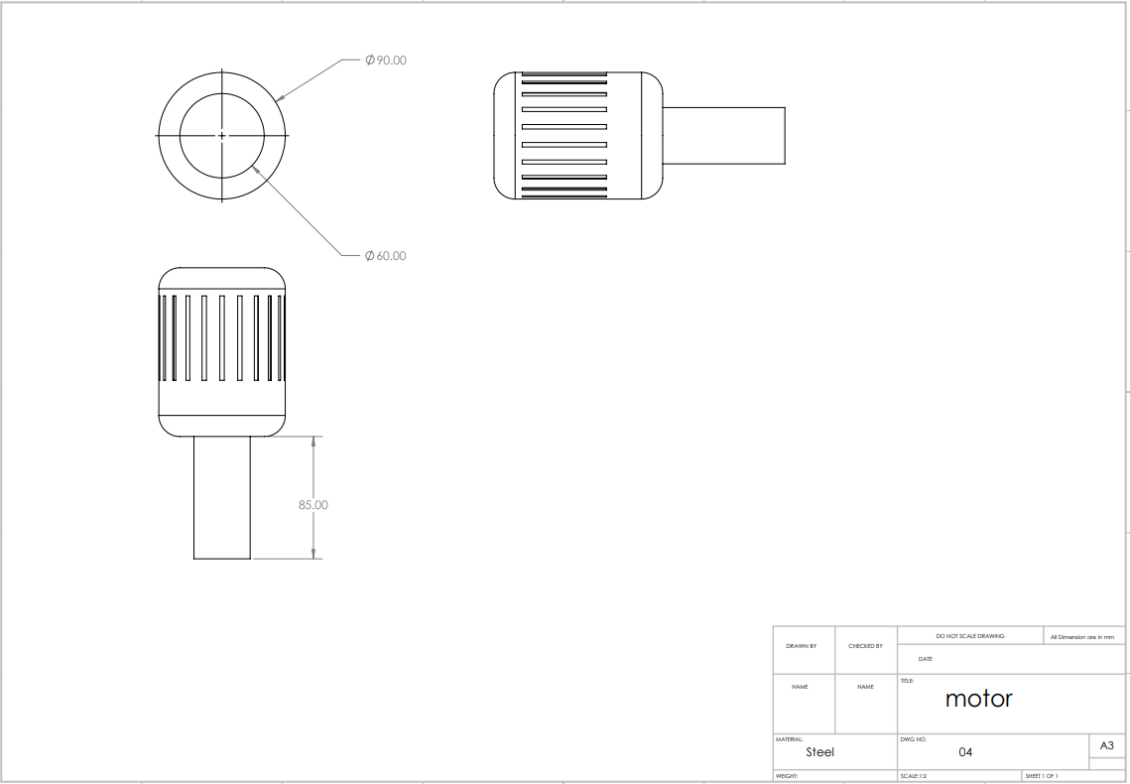
- Maneka Sanjay Gandhi. (2014, July 13). Manure happens. Kathmandu, Nepal: The Kathmandu Post. Retrieved from <https://kathmandupost.com/opinion/2014/07/13/manure-happens#:~:text=Cattle%20manure%20contains%20an%20average,phosphorus%20and%2032%20other%20micronutrients.>
- Morath Benjamin. (2023). *Designing a small-scale screw press for blackwater dewatering*. ETH Zurich.
- Muhammad Firdaus et. al. (2017). Preliminary Design on Screw Press Model of Palm Oil. *IOP Conference Series: Materials Science and Engineering* 165. IOP Publishing.
- Okafor, Basil E. (2015). Development of Palm Oil Extraction System. *International Journal of Engineering and Technology*, 5, 68-75.
- P. Y. Sherpa, P. Sharma & R. Panthi. (2017). *End Use Diversification of Biogas Plant Through Design Fabrication And Testing of Prototype Biogas Slurry Dewatering Machine For Mass Dissemination In Nepal*. Lalitpur, Nepal: Tribhuwan University, Institute Of Engineering, Pulchowk Campus, Department Of Mechanical Engineering.
- P. Y. Sherpa, P. Sharma and R. Panthi. (2017). *End Use Diversification of Biogas Plant Through Design Fabrication And Testing of Prototype Biogas Slurry Dewatering Machine For Mass Dissemination In Nepal*. Lalitpur, Nepal: Department of Mechanical and Aerospace Engineering, IOE.
- Riedel D. J. (2009). *An Investigation into the Mechanisms of Sludge Reduction Technologies*. .
- Sujan Jojju. (2023). *Design, Fabrication and Performance Evaluation of The Dewatering Machine or Bio-Digestate*. LALITPUR, NEPAL: DEPARTMENT OF MECHANICAL AND AEROSPACE ENGINEERING, IOE .
- Velkushanova K. Strande L. & Ronteltap M. (2021). *Methods for Faecal Sludge Analysis*. London, UK.: IWA Publishing.

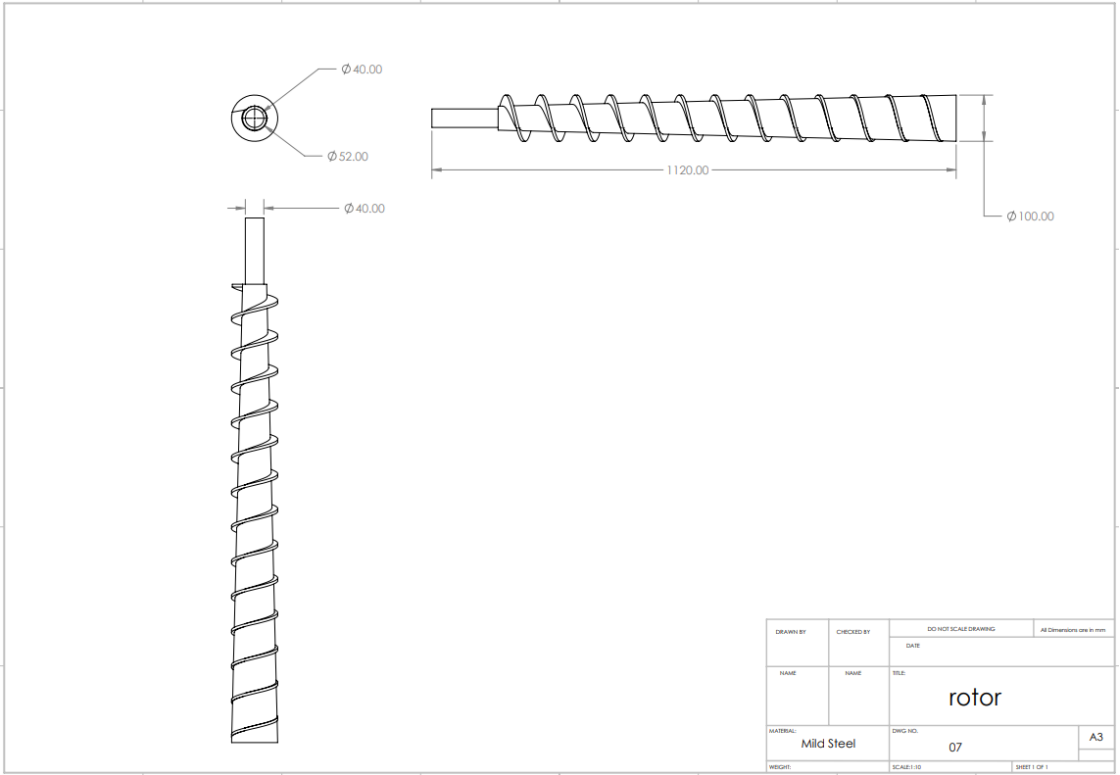
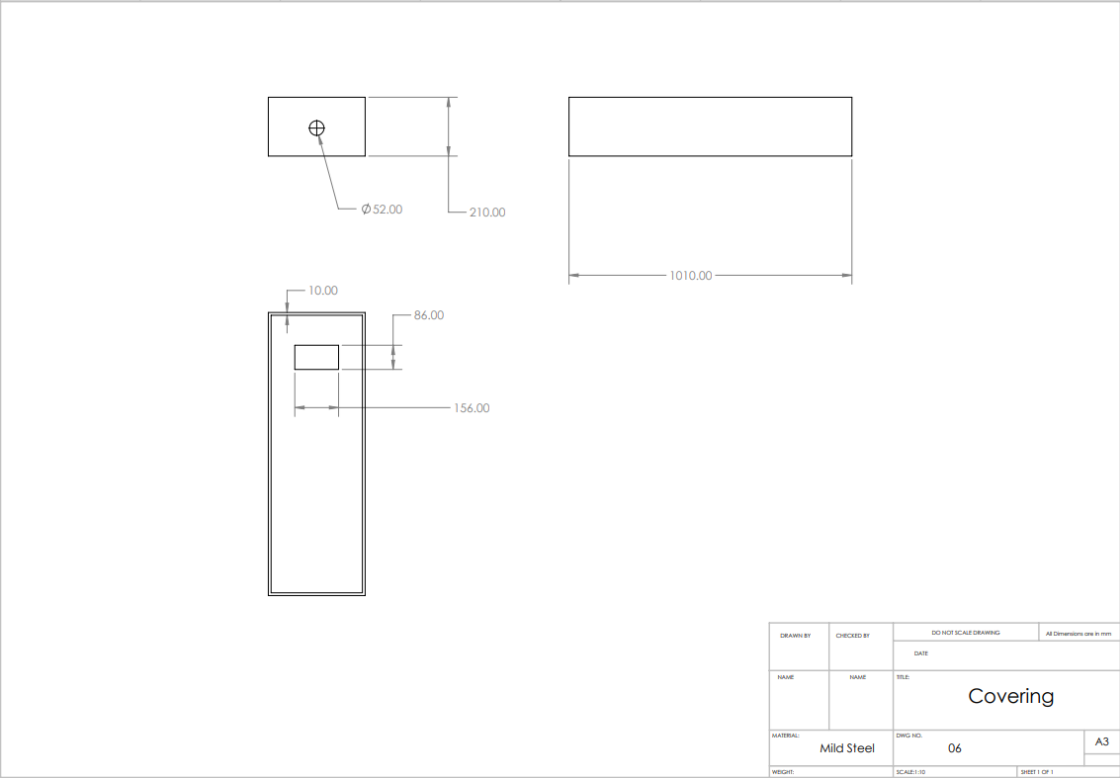
ANNEXES

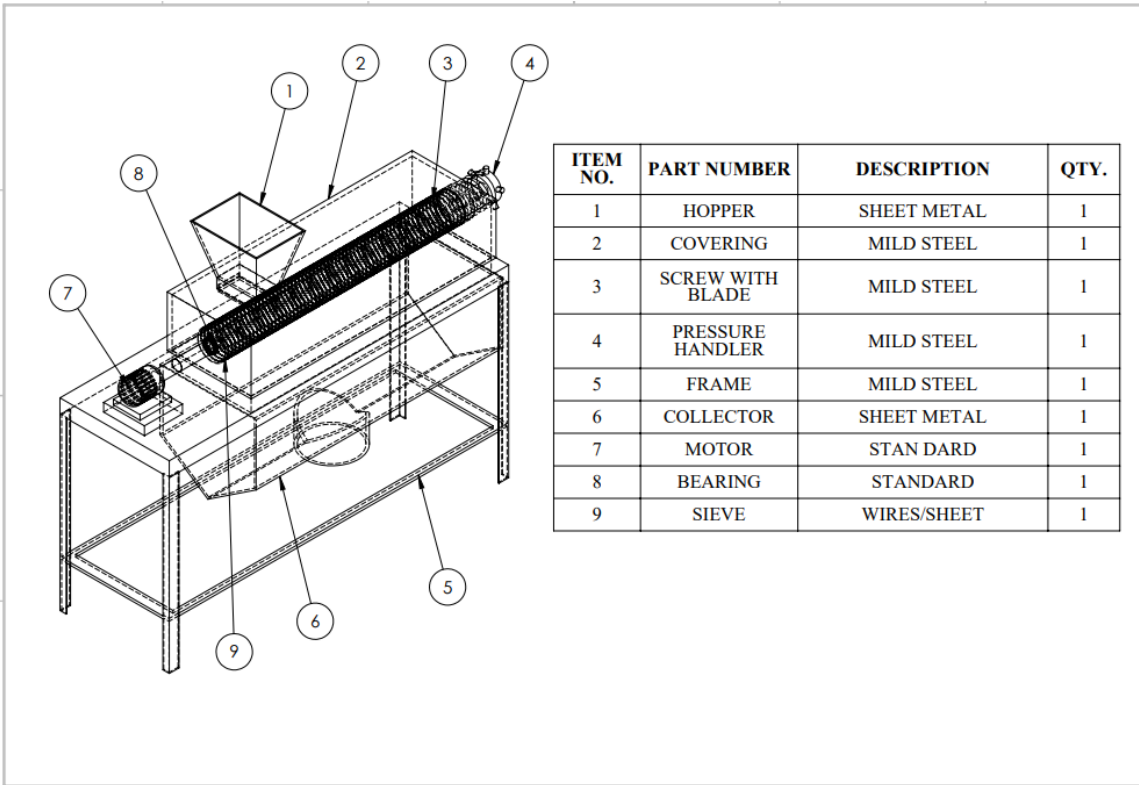
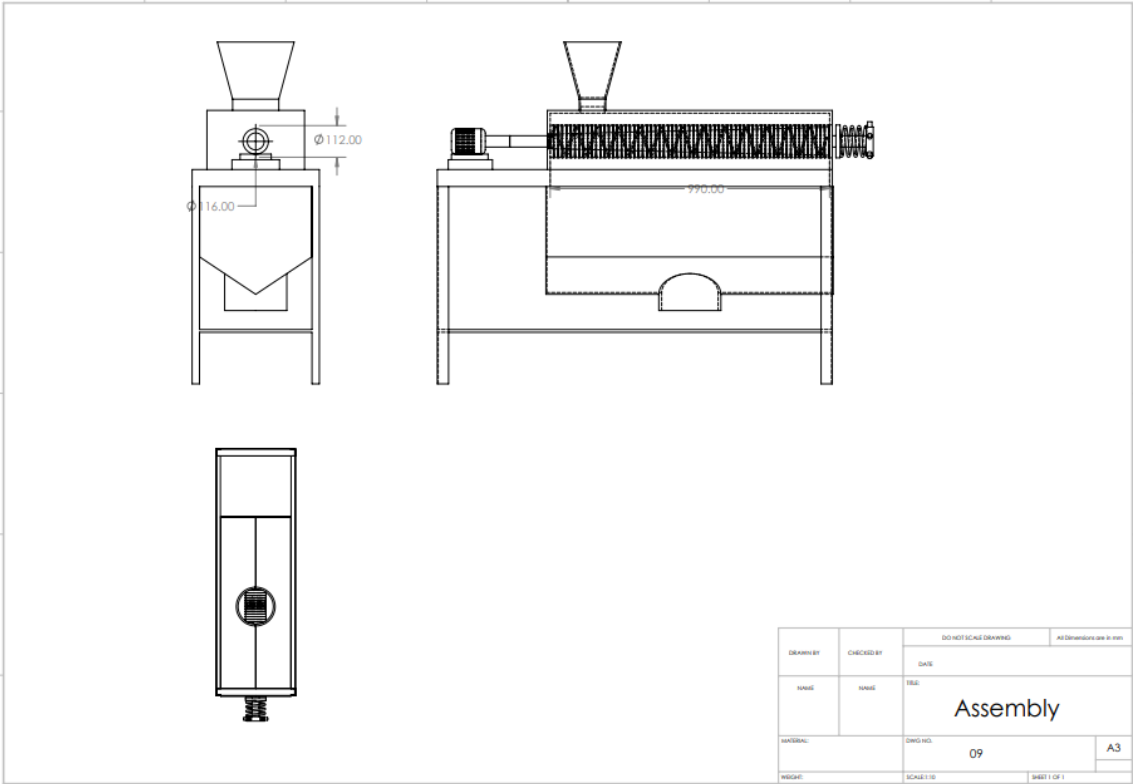
Parts of Dewatering Machine with detailed dimensions











BOM, Bill of Materials

Details of "Mesh"

<input type="checkbox"/> Relevance	0
Element Order	Program Controlled
- Sizing	
Size Function	Adaptive
Relevance Center	Fine
<input type="checkbox"/> Element Size	Default
Initial Size Seed	Assembly
Transition	Fast
Span Angle Center	Fine
Automatic Mesh ...	On
<input type="checkbox"/> Defeature Size	Default
Minimum Edge L...	6.0 mm
+ Quality	
+ Inflation	
+ Advanced	
- Statistics	
<input type="checkbox"/> Nodes	22669
<input type="checkbox"/> Elements	11951

Mesh details

Outline of Schematic F2, G2, H2, I2: Engineering Data				
	A	B	C	D
1	Contents of Engineering Data			Source
2	Material			Description
3	Structural Steel		General_Materials.xml	Fatigue Data at zero mean stress comes from 1998 ASME BPV Code, Section 8, Div 2, Table 5-110.1

Properties of Outline Row 3: Structural Steel				
	A	B	C	E
1	Property	Value	Unit	
2	Material Field Variables	Table		
3	Density	7850	kg m^-3	
4	Isotropic Secant Coefficient of Thermal Expansion			
5	Coefficient of Thermal Expansion	1.2E-05	C^-1	
6	Isotropic Elasticity			
7	Derive from	Young's Modulus and Poisson...		
8	Young's Modulus	2E+11	Pa	
9	Poisson's Ratio	0.3		
10	Bulk Modulus	1.6667E+11	Pa	
11	Shear Modulus	7.6923E+10	Pa	
12	Alternating Stress Mean Stress	Tabular		
16	Strain-Life Parameters			
17	Display Curve Type	Strain-Life		
18	Strength Coefficient	9.2E+08	Pa	
19	Strength Exponent	-0.106		
20	Ductility Coefficient	0.213		
21	Ductility Exponent	-0.47		
22	Cyclic Strength Coefficient	1E+09	Pa	
23	Cyclic Strain Hardening Exponent	0.2		
24	Tensile Yield Strength	2.9E+08	Pa	
25	Compressive Yield Strength	2.9E+08	Pa	
26	Tensile Ultimate Strength	4.6E+08	Pa	
27	Compressive Ultimate Strength	0	Pa	

Material properties in ANSYS

Mass-Flow Inlet

Zone Name

Momentum Thermal Radiation Species DPM Multiphase Potential UDS

Reference Frame Absolute

Mass Flow Specification Method Mass Flow Rate

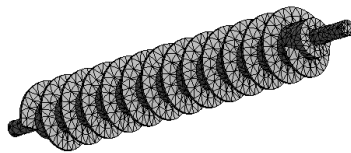
Mass Flow Rate (kg/s) 0.55 constant

Supersonic/Initial Gauge Pressure (pascal) 0 constant

Direction Specification Method Normal to Boundary

OK Cancel Help

Mass flow rate

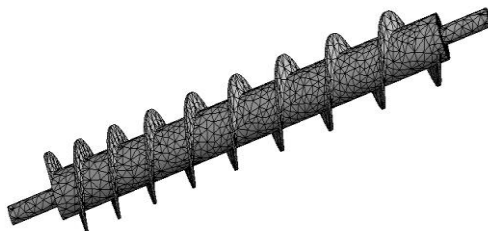


Meshed figure for Constant Pitch Screw with Straight shaft

F: Static Structural
Static Structural
Time: 1. s
A Moment: 3.e+005 N.mm
B Fixed Support

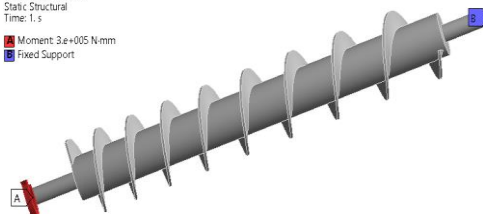


Boundary Conditions for Constant Pitch Screw with Straight shaft



Meshed figure for Variable pitch screw with Straight shaft

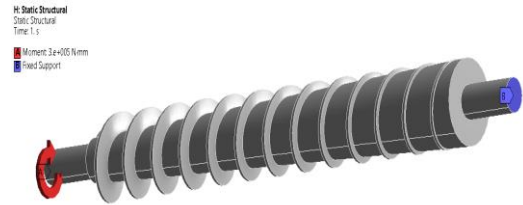
G: Static Structural
Static Structural
Time: 1. s
A Moment: 3.e+005 N.mm
B Fixed Support



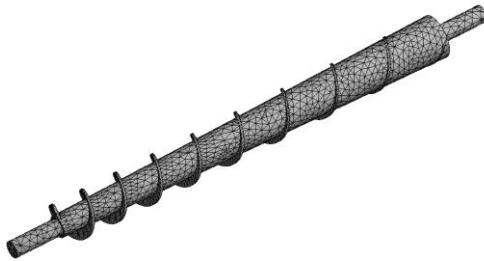
Boundary Conditions for Variable pitch screw with Straight shaft



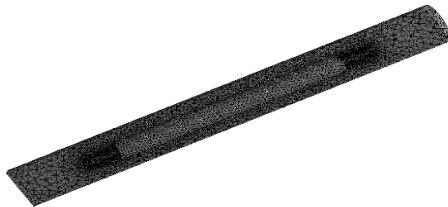
Meshed Figure for Constant Pitch Screw
with Tapered Shaft



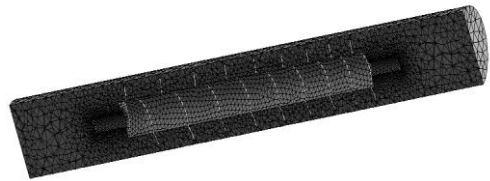
Boundary Conditions for Constant Pitch
Screw with Tapered Shaft



Meshed figure for Variable Pitch Screw
with Tapered Shaft



Fluid Flow Domain for Constant Pitch
Screw with Straight shaft



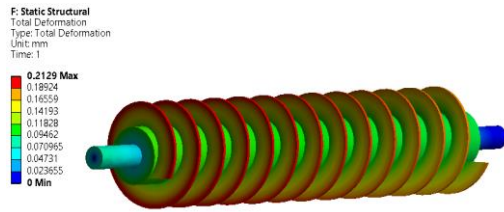
Fluid Domain for variable pitch screw
with Straight shaft



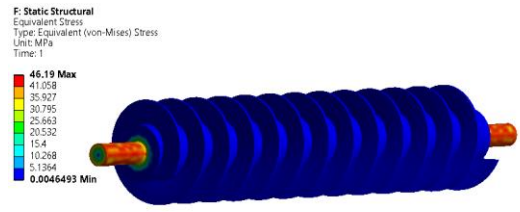
Fluid Domain for Constant Pitch Screw
with Tapered Shaft



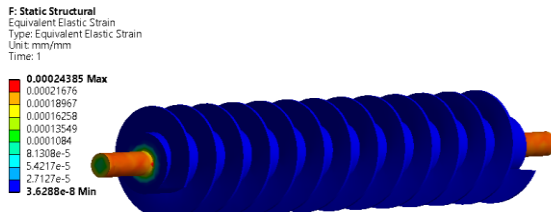
Fluid Domain with mesh for Variable Pitch
Screw with Tapered Shaft



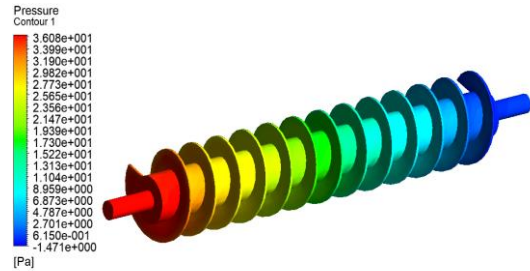
Total Deformation at Constant Pitch
Screw with Straight shaft



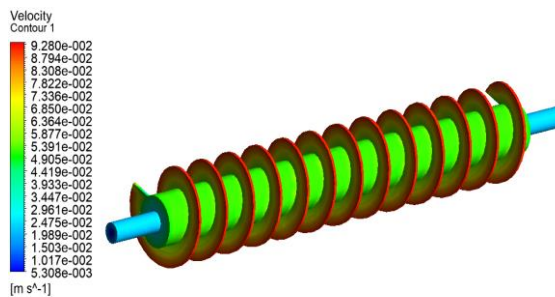
Equivalent Stress on Constant Pitch
Screw with Straight shaft



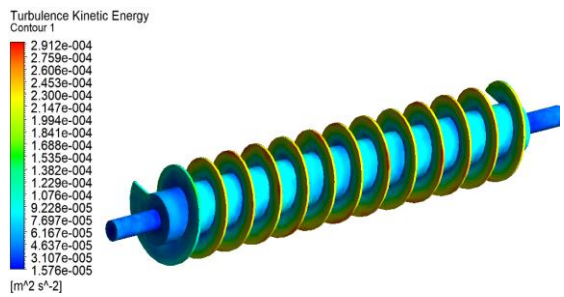
Equivalent strain on Constant Pitch Screw
with Straight shaft



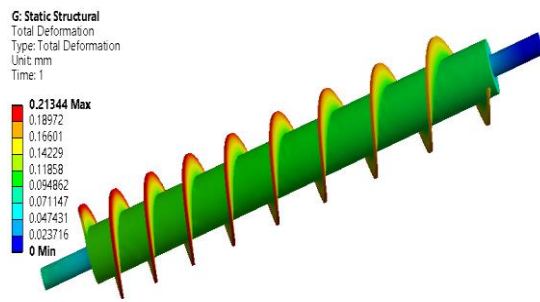
Pressure Contour for Constant Pitch
Screw with Straight shaft



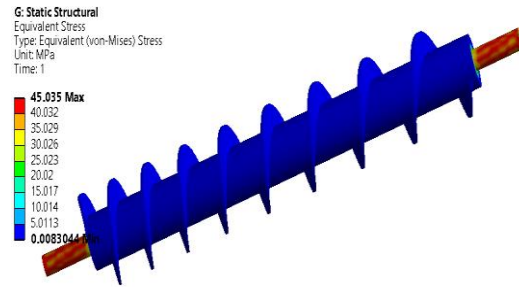
Velocity Contour for Constant Pitch Screw
with Straight shaft



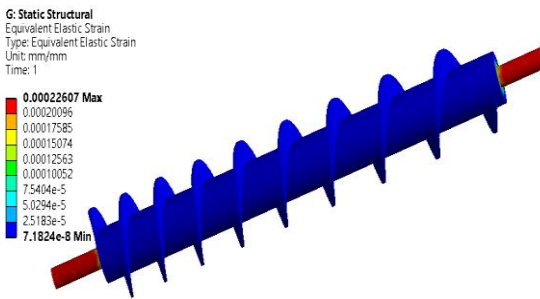
TKE for Constant Pitch Screw with
Straight shaft



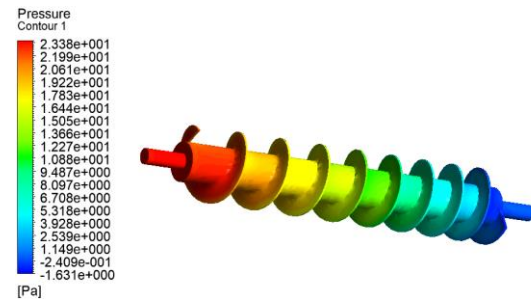
Total Deformation at Variable pitch screw
with Straight shaft



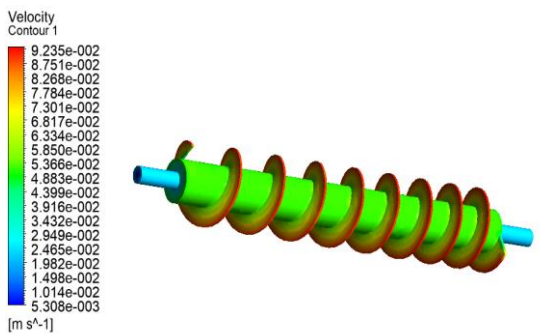
Equivalent Stress on Variable pitch screw
with Straight shaft



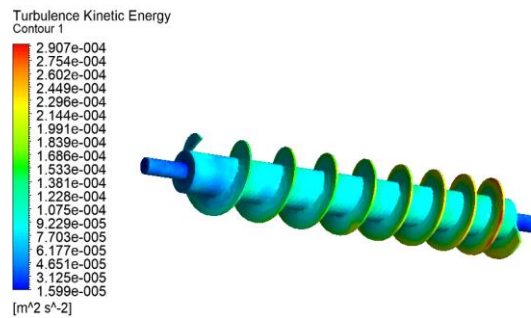
Equivalent Strain on Variable pitch screw
with Straight shaft



Pressure Contour for Variable pitch screw
with Straight shaft

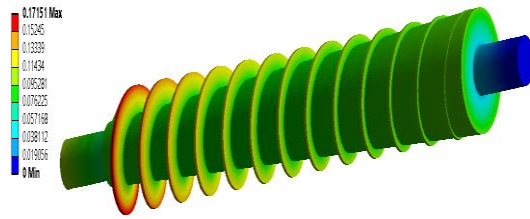


Velocity Contour for Variable pitch screw
with Straight shaft



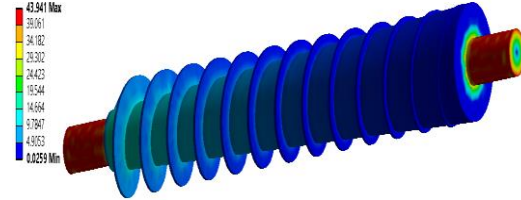
TKE for Variable pitch screw with
Straight shaft

H: Static Structural
Total Deformation
Type: Total Deformation
Unit: mm
Time: 1



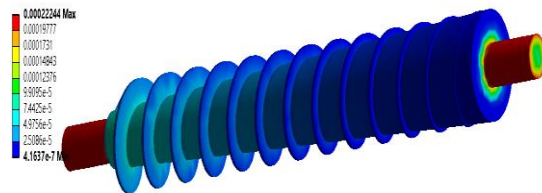
Total deformation at Constant Pitch Screw
with Tapered Shaft

H: Static Structural
Equivalent Stress
Type: Equivalent (von-Mises) Stress
Unit: MPa
Time: 1



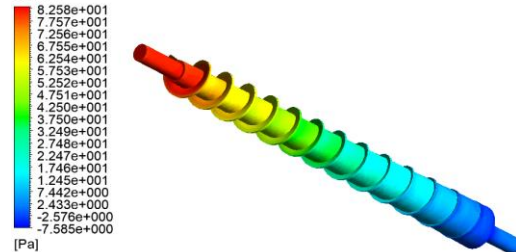
Equivalent Stress on Constant Pitch
Screw with Tapered Shaft

H: Static Structural
Equivalent Elastic Strain
Type: Equivalent Elastic Strain
Unit: mm/mm
Time: 1



Equivalent Strain on Constant Pitch Screw
with Tapered Shaft

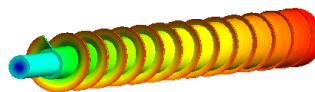
Pressure
Contour 1
[Pa]



Pressure Contour for Constant Pitch
Screw with Tapered Shaft

Velocity
Contour 1

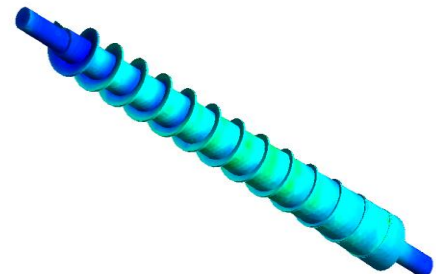
5.135e-002
4.679e-002
4.624e-002
4.368e-002
4.112e-002
3.856e-002
3.600e-002
3.345e-002
3.089e-002
2.833e-002
2.577e-002
2.321e-002
2.066e-002
1.810e-002
1.554e-002
1.298e-002
1.042e-002
7.866e-003
5.308e-003
[m s⁻¹]



Velocity Contour for Constant Pitch Screw
with Tapered Shaft

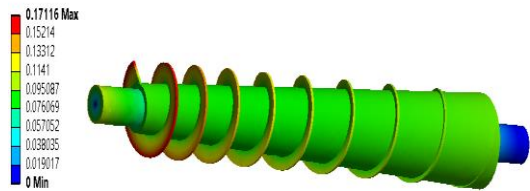
Turbulence Kinetic Energy
Contour 1

1.907e-003
1.802e-003
1.698e-003
1.593e-003
1.488e-003
1.384e-003
1.279e-003
1.175e-003
1.070e-003
9.654e-004
8.608e-004
7.562e-004
6.516e-004
5.470e-004
4.424e-004
3.378e-004
2.332e-004
1.286e-004
2.399e-005
[m² s⁻²]



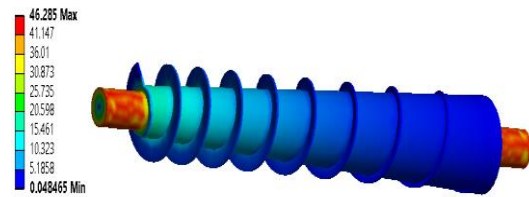
TKE for Constant Pitch Screw with
Tapered Shaft

I: Static Structural
Total Deformation
Type: Total Deformation
Unit: mm
Time: 1



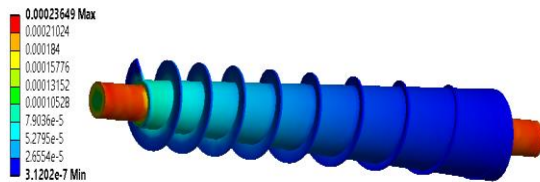
Total Deformation at Variable Pitch Screw
with Tapered Shaft

I: Static Structural
Equivalent Stress
Type: Equivalent (von-Mises) Stress
Unit: MPa
Time: 1



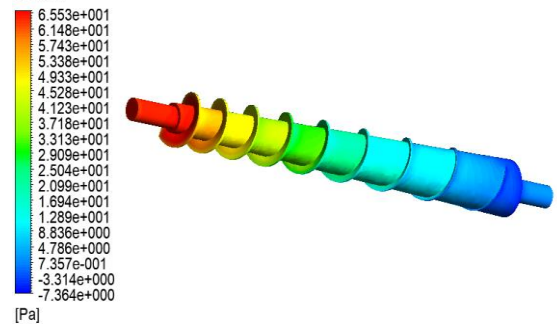
Equivalent Stress on Variable Pitch
Screw with Tapered Shaft

I: Static Structural
Equivalent Elastic Strain
Type: Equivalent Elastic Strain
Unit: mm/mm
Time: 1



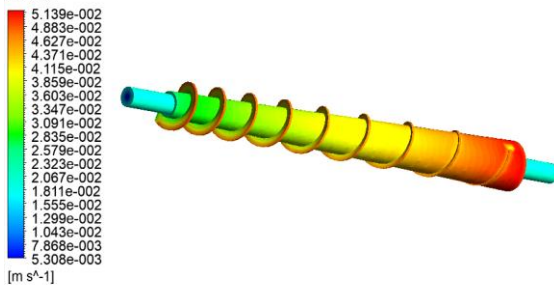
Equivalent Strain on Variable Pitch Screw
with Tapered Shaft

Pressure
Contour 1



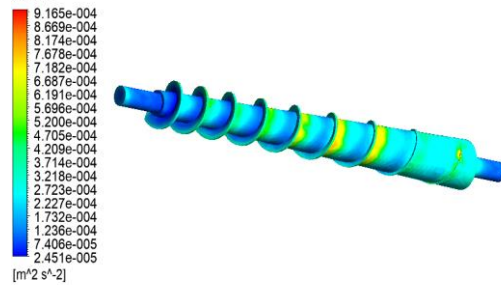
Pressure Contour for Variable Pitch
Screw with Tapered Shaft

Velocity
Contour 1



Velocity Contour for Variable Pitch Screw
with Tapered Shaft

Turbulence Kinetic Energy
Contour 1



TKE for Variable Pitch Screw with
Tapered Shaft



Motor drive with screw press



Complete fabricated system with pressure cone



Sample Collection



pH mesurement for the sample before and after sundrying



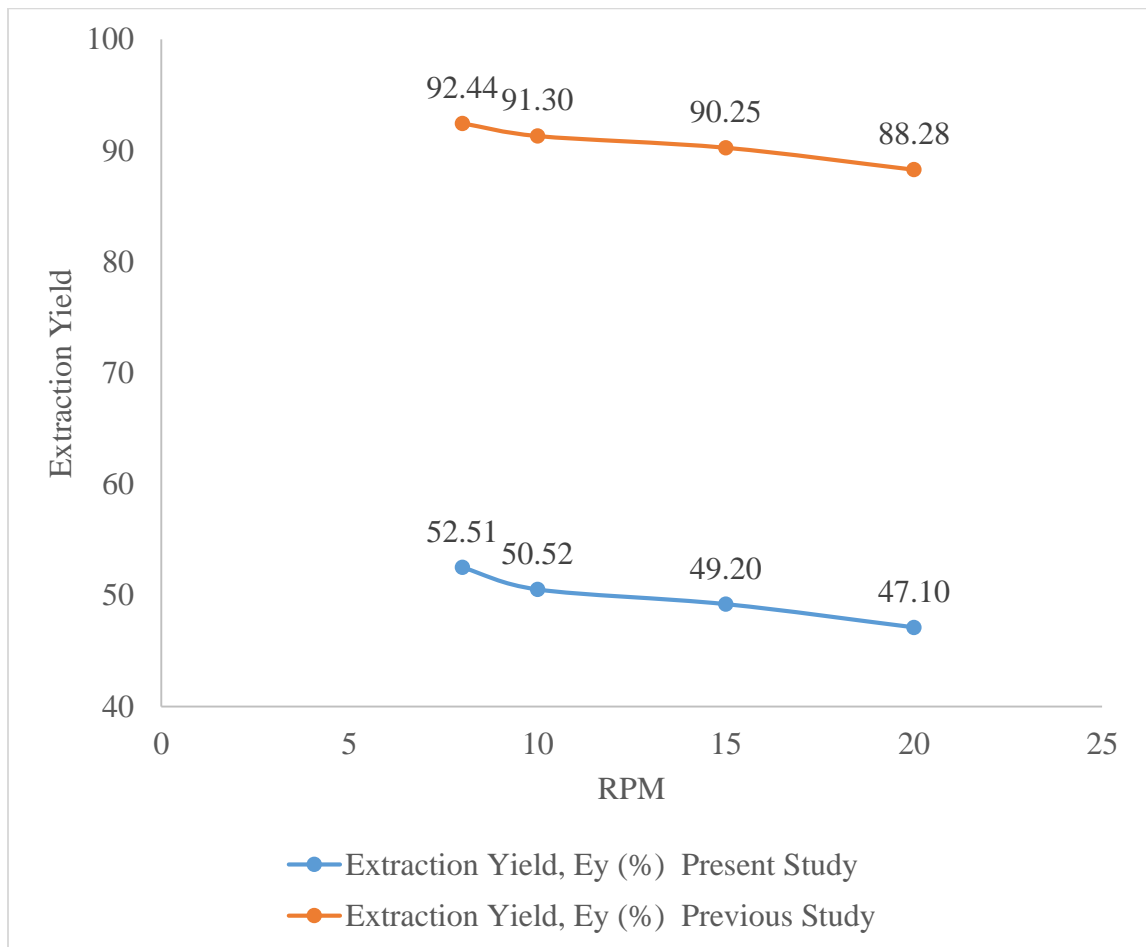
pH mesurement for the pretreatment of sample before dewatering



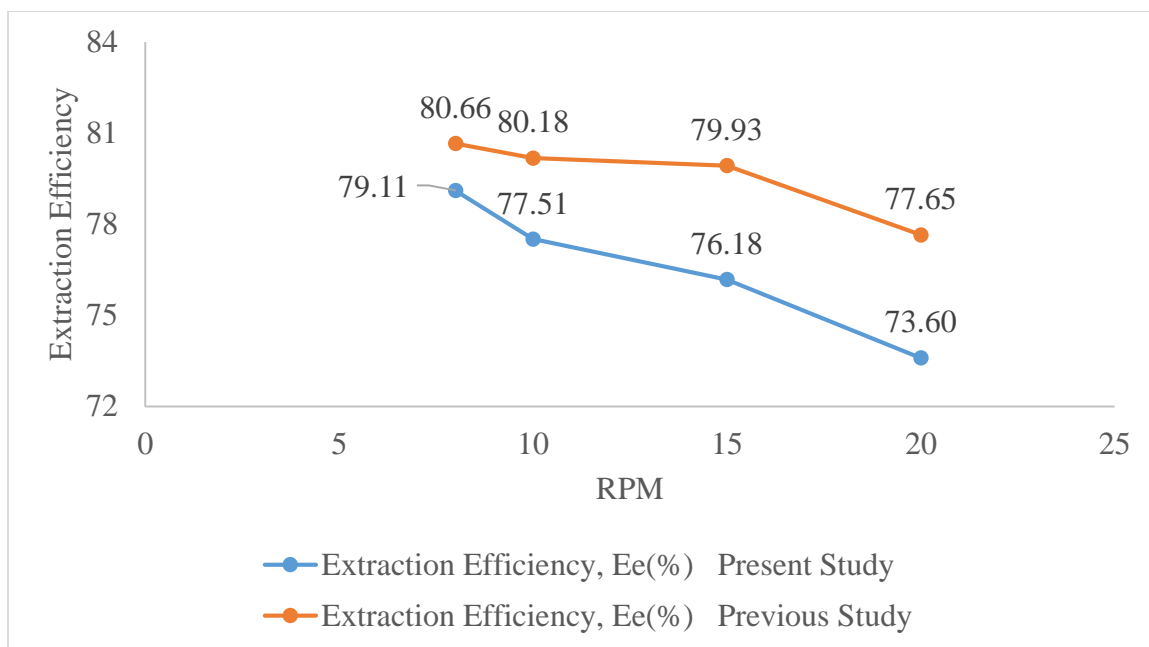
VFD with complete assembled dewatering machine



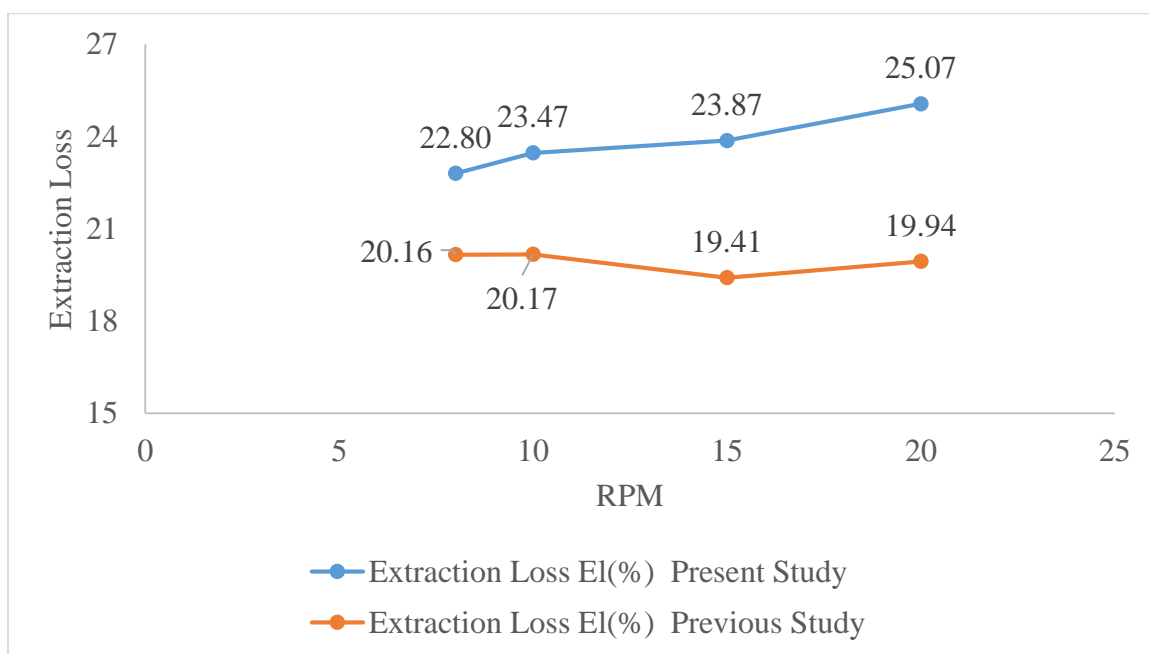
Assembling work on dewatering machine



Comparison of Extraction Yield with Previous Data



Comparison of Extraction Efficiency with Previous Data



Comparison of Extraction Loss with Previous Data

Design and Improvement of Dewatering System Implemented for Biogas Slurry

ORIGINALITY REPORT

6%

SIMILARITY INDEX

PRIMARY SOURCES

1	assets.researchsquare.com Internet	182 words — 3%
2	dspace.alquds.edu Internet	34 words — 1%
3	hdl.handle.net Internet	21 words — < 1%
4	doaj.org Internet	18 words — < 1%
5	envirosim.com Internet	17 words — < 1%
6	5dok.net Internet	15 words — < 1%
7	Ton Duc Thang University Publications	14 words — < 1%
8	Madhuri More, Chitranjan Agrawal, Deepak Sharma. "Chapter 20 Development of Screw Press-Dewatering Unit for Biogas Slurry", Springer Science and Business Media LLC, 2023 Crossref	13 words — < 1%

9	www.researchgate.net Internet	11 words — < 1%
10	docs.assets.eco.on.ca Internet	10 words — < 1%
11	www.coursehero.com Internet	10 words — < 1%
12	1library.net Internet	9 words — < 1%

EXCLUDE QUOTES ON
EXCLUDE BIBLIOGRAPHY ON

EXCLUDE SOURCES < 6 WORDS
EXCLUDE MATCHES < 9 WORDS



International Journal For Multidisciplinary Research

An International Open Access Peer Reviewed Journal

E-ISSN: 2582-2160

Certificate of Publication

The editorial board of IJFMR is hereby awarding the certificate of publication to

Sunil Yadav

in recognition of publication of paper titled

Design and Improvement of Dewatering System Implemented for Biogas Slurry

Published In: Volume 5, Issue 6 (November-December 2023)

Paper Id: 9184

www.ijfmr.com • editor@ijfmr.com

A handwritten signature in blue ink, appearing to read 'GyB', is positioned above the Editor/Publisher text.

Editor / Publisher

IJFMR